S-NPP ATMS: Antenna Temperature (TDR) Conversion to Brightness Temperature (SDR)

ATMS SDR Team

Vince Leslie MIT LL (Presenter)

Suomi NPP SDR Science and Product Review

18 December 2013

College Park, MD

This work was sponsored by the National Oceanic and Atmospheric Administration under contract FA8721-05-C-0002. Opinions, interpretations, conclusions, and recommendations are those of the author and are not necessarily endorsed by the United States Government.

Outline

- TDR-to-SDR Conversion Objective
- Team's Conversion Approach
- ATMS SDR Algorithm Implementation
- Verification Results
  - CRTM & NWP/GPS-RO dataset
  - NAST-M aircraft observations
  - CRTM & ECMWF dataset
- Analysis of the S-NPP Pitchover Maneuver Scan Bias
- Path Forward

Objective

- The ATMS Temperature Data Record (TDR), i.e., the antenna temperature, is converted to a Sensor Data Record (SDR), i.e., the brightness temperature
- The general TDR-to-SDR relationship for microwave radiometers is

Brightness temperature of the scene

Antenna Temperature measured by the radiometer

$$T_A = \frac{1}{4\pi} \int_{4\pi} G(\theta,\phi) \cdot T_B(\theta,\phi)\, d\Omega$$

Steradian or solid angle

Antenna pattern

- Other contributions include polarization twist, ant. pattern spillover, and sensor self emission
- The objective is to express and then invert the above relationship to convert the measured TDR into an SDR using first principles:
  – Antenna pattern measurements made in a Compact Antenna Test Range
  – S-NPP spacecraft pitchover maneuver data
  – Assumptions of the radiometric environment

Approximating the ATMS TDR-to-SDR Relationship

Contributions to the TDR:

a) Main lobe
b) Side lobe viewing the Earth
c) Side lobe viewing deep space
d) Near-field satellite radiation

Quasi-Vertical pol. Vertical pol. Horizontal pol.

$$T_b^{Qv} = T_b^{v} \cos^2\theta + T_b^{h} \sin^2\theta$$

Scan angle

$$\underset{\text{TDR}}{T_a^{Qv}} = \overbrace{\eta_{me}^{vv} T_b^{Qv} + \eta_{me}^{hv} T_b^{Qh}}^{a} + \overbrace{\eta_{se}^{vv} E_b^{Qv} + \eta_{se}^{hv} E_b^{Qh}}^{b} + \underbrace{\eta_{sc}^{vv} C_b^{Qv} + \eta_{sc}^{hv} C_b^{Qh}}_{c} + \underset{d}{S_a^{Qv}}$$

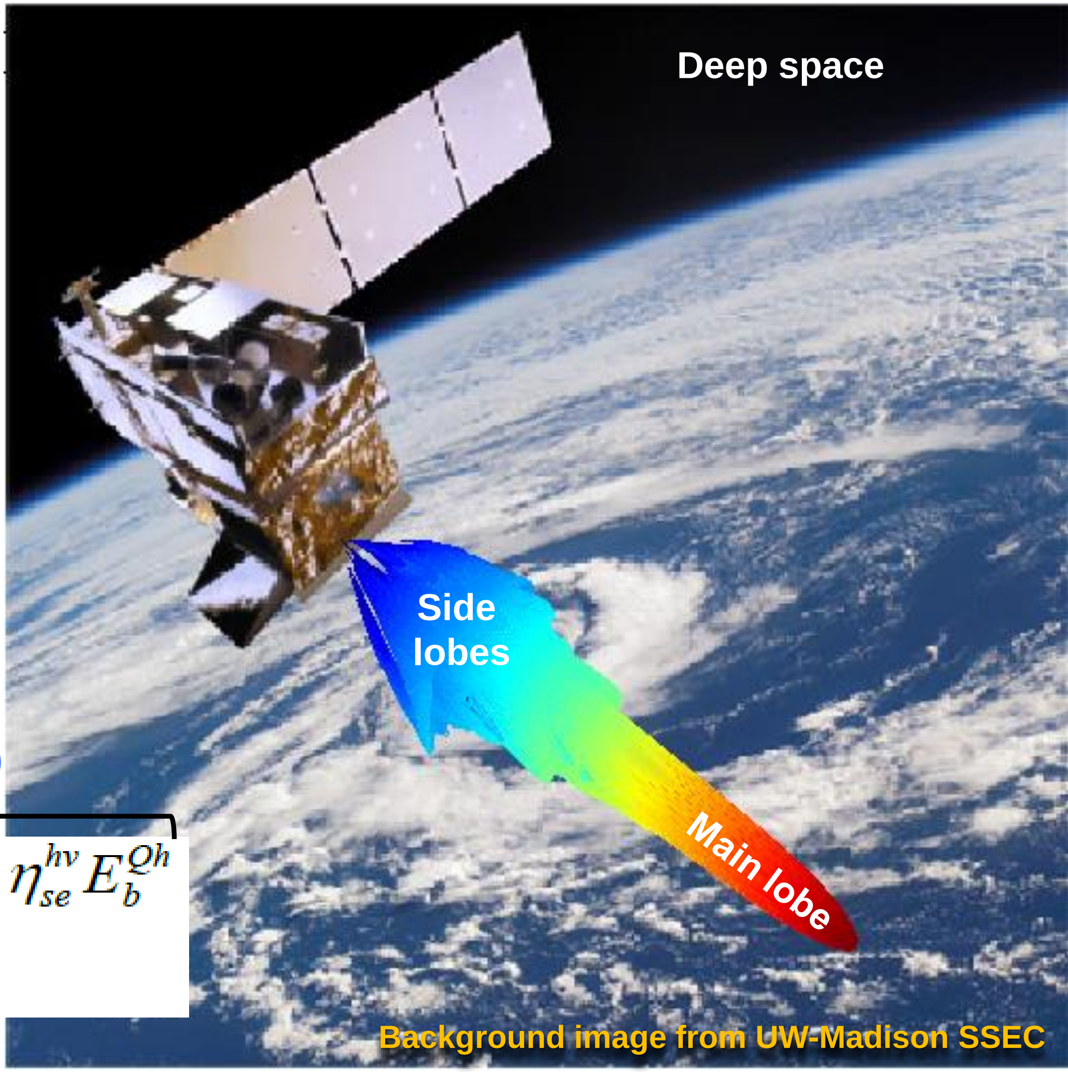

S-NPP Eta Derivation

- **Used S-NPP ATMS antenna pattern measurements made in CATR**
- **Main lobe was 2.5x the channel's beamwidth**
- **S-NPP G-band did not have enough dynamic range in CATR to properly calculate beam efficiency (fixed for J1)**
- **W-band had a high cross-pol. antenna pattern**

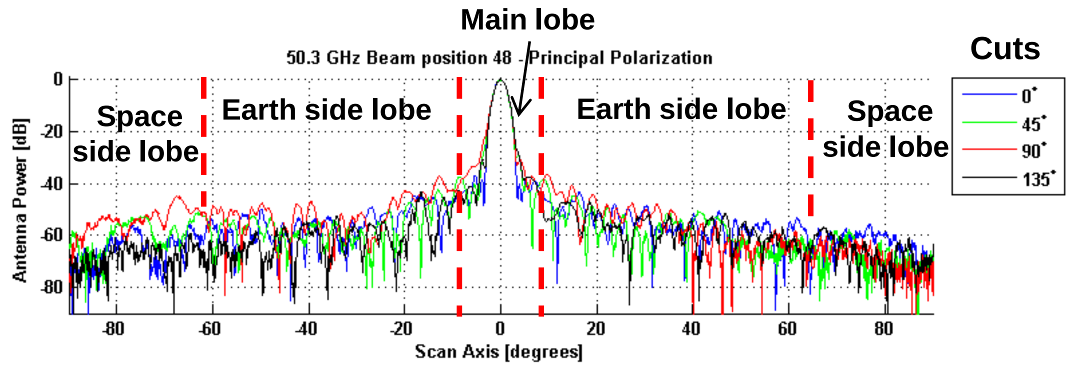

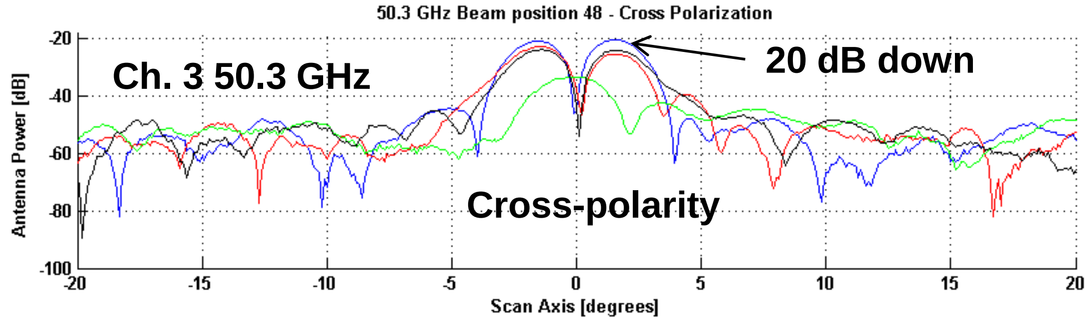

	Principal or Co			**Cross**		
Ch.	$\eta_{me}^{pp}+\eta_{se}^{pp}$ (%)			$\eta_{me}^{pq}+\eta_{se}^{pq}$ (%)		
	B1	B48	B96	B1	B48	B96
1	97.82	98.44	97.89	1.40	1.27	1.16
2	98.52	98.62	98.38	0.99	1.02	0.86
3	97.94	98.06	98.08	1.46	1.56	1.33
4	98.10	98.19	98.40	1.38	1.39	1.03
5	98.10	98.15	97.91	1.35	1.41	1.37
6	98.07	98.20	97.89	1.32	1.45	1.48
7	98.18	98.29	98.25	1.30	1.30	1.15
8	98.20	98.24	97.76	1.27	1.36	1.57
9	98.30	98.37	98.25	1.24	1.30	1.20
10	98.47	98.59	98.34	1.19	1.19	1.19
11	98.47	98.59	98.34	1.19	1.19	1.19
12	98.47	98.59	98.34	1.19	1.19	1.19
13	98.47	98.59	98.34	1.19	1.19	1.19
14	98.47	98.59	98.34	1.19	1.19	1.19
15	98.47	98.59	98.34	1.19	1.19	1.19

W- & G-band channels did not use the antenna pattern measurements to convert TDR to SDR

Ch.	$\eta_{me}^{pp}+\eta_{se}^{pp}+\eta_{me}^{pq}+\eta_{se}^{pq}$ (%)		
	B1	B48	B96
16	1.00	1.00	1.00
17	1.00	1.00	1.00
18	1.00	1.00	1.00
19	1.00	1.00	1.00
20	1.00	1.00	1.00
21	1.00	1.00	1.00
22	1.00	1.00	1.00

S-NPP vs J1 G-band CATR Measurements

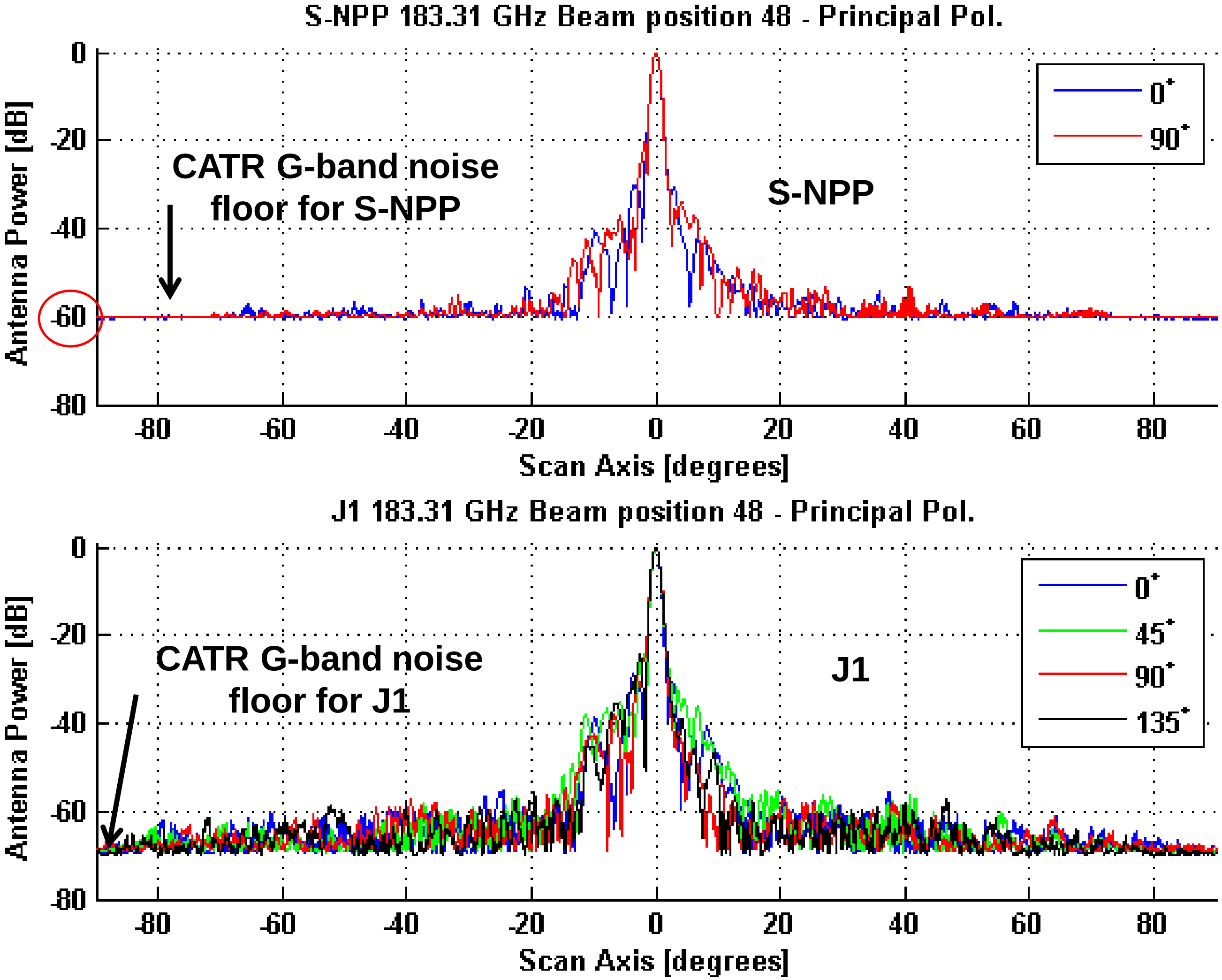

- **SDR team has several options for S-NPP**
- **Option 1: don't use the S-NPP measurements**
- **Option 2: model the side lobes under the noise floor**
- **Option 3: replace the S-NPP measurements under the noise floor with the J1 measurements**

Near-field Satellite Radiation

- S-NPP spacecraft pitchover maneuver showed an unexpected result
- The homogenous unpolarized cosmic background radiation was not flat across scan angle
- For the TDR-to-SDR conversion, this was attributed to near-field satellite contamination (other explanations discussed later)

$$S_a^{QV} = \beta_0^v + \beta_1^v \cdot \sin^2(\theta)$$
$$S_a^{QH} = \beta_0^h + \beta_1^h \cdot \cos^2(\theta)$$

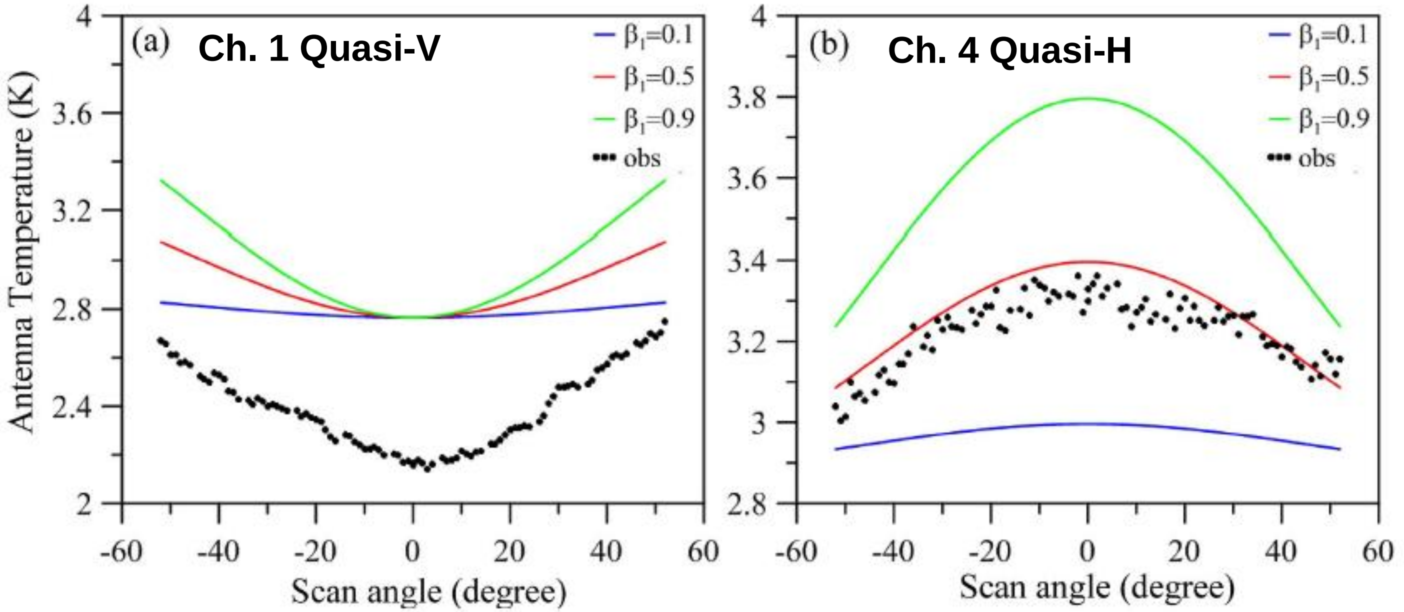

Channel	β_0	β_1
1	0.0553	0.8123
2	0.0389	0.7167
3	0.0460	0.3781
4	-0.0010	0.4499
5	0.0527	0.3877
6	0.0144	0.4520
7	0.0730	0.4503
8	0.1133	0.4517
9	0.1049	0.4558
10	0.1419	0.5474
11	0.1271	0.5199
12	0.1675	0.4969
13	0.1190	0.5213
14	0.1187	0.5283
15	0.1583	0.6107
16	0.0065	1.1983
17	-0.0697	0.7106
18	-0.1200	0.9832
19	-0.0623	0.8911
20	-0.0525	0.8986
21	-0.0147	0.8773
22	-0.0689	1.0274

Implementing the Conversion in the Operational Code

IDPS Code Framework

SDR = BeamEffCorr x TDR + ScanBias

- **The IDPS ATMS SDR Algorithm has a simple linear conversion from antenna temperature to brightness temperature**
- **BeamEffCorr is the multiplicative conversion factor for each channel and beam position (22 x 96)**
- **ScanBias is the additive conversion factor for each channel and beam position (22 x 96)**
- **Operational code does not distinguish between land/ocean surfaces, but it is a proposed enhancement to match NOAA heritage data products**

Latest Coefficients in Operational PCT

$$\text{BeamEffCorr} = \frac{1 - a \times \eta_{me}^{cr}}{\eta_{me}^{co} + \eta_{se}^{co} + \eta_{se}^{cr}} \qquad \text{ScanBias} = -\frac{S_a + b \times \eta_{me}^{cr}}{\eta_{me}^{co} + \eta_{se}^{co} + \eta_{se}^{cr}}$$

ATMS Channel	BeamEffCorr	ScanBias	a	b
1 – 5	See above	See above	regressed	regressed
6 - 15	See above	See above	1	0
16 - 22	1	-Sa	N/A	N/A

Example Correction Coefficients

Beam Efficiency Correction (Multiplicative)

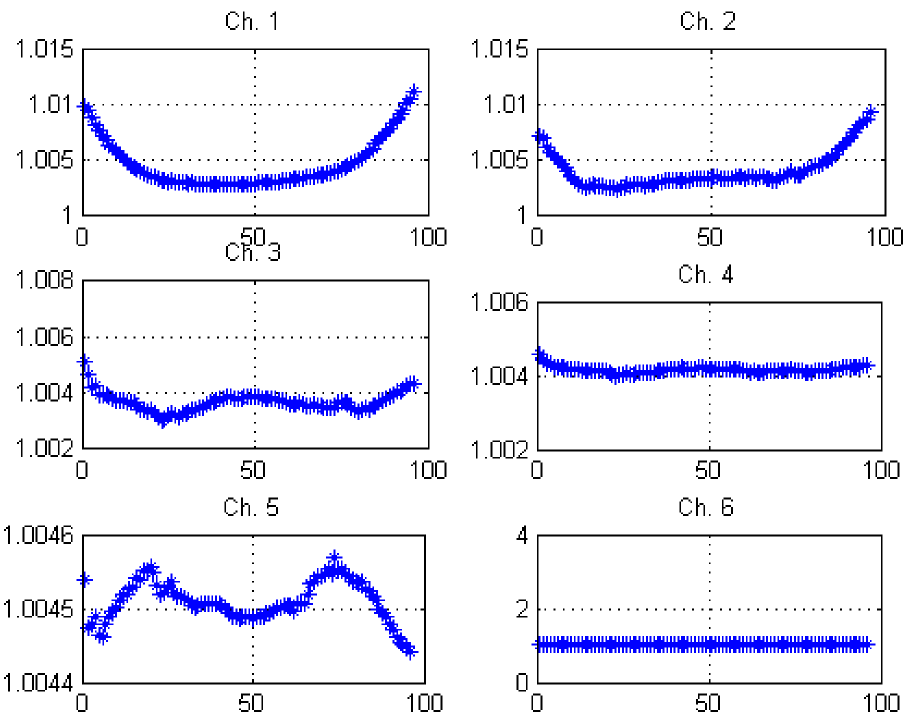

Beam Position

Beam Position

Scan Bias Correction (Kelvin)

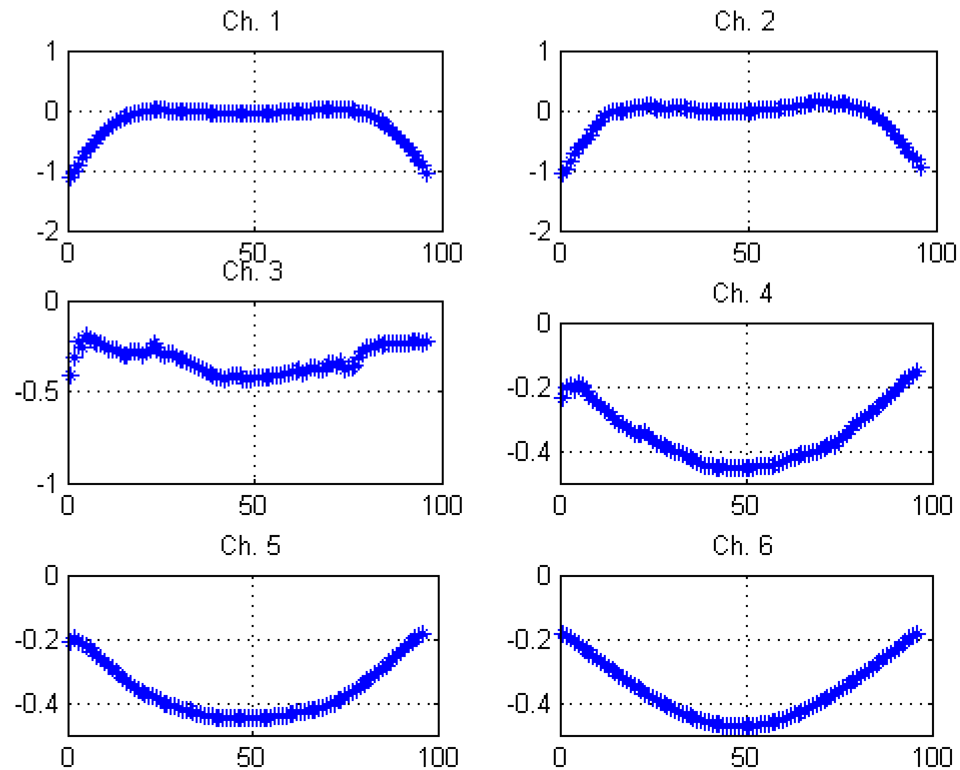

Beam Position

Beam Position

Verification Results

CRTM & GFS/GPS-RO

- Validation datasets used CRTM simulations using GFS (mainly for window channels) and GPS RO (mainly for sounding channels) as inputs
- Clear skies where determined using ATMS Cloud Liquid Water retrievals (< 0.03 g/cm^3)
- Collocated COSMIC GPS RO
  - +/- 60° latitude
  - Dec. 10, 2011 to March 31, 2013
  - About 3000 collocated measurements/month
- NWP dataset
  - GFS 64-level forecasts
  - December 20-26 2012 (7 days)

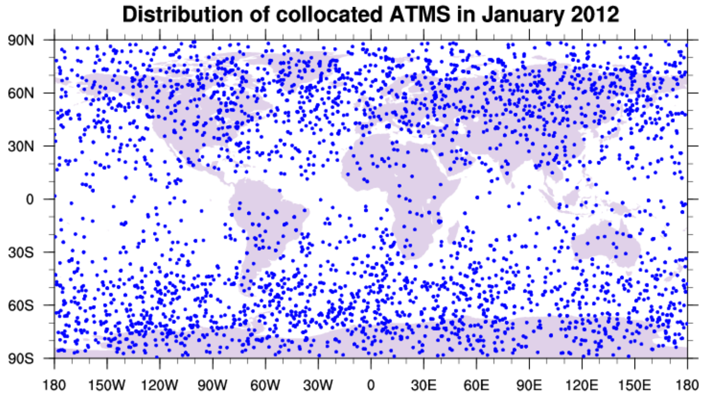

GPS-RO

CRTM & GFS/GPS-RO

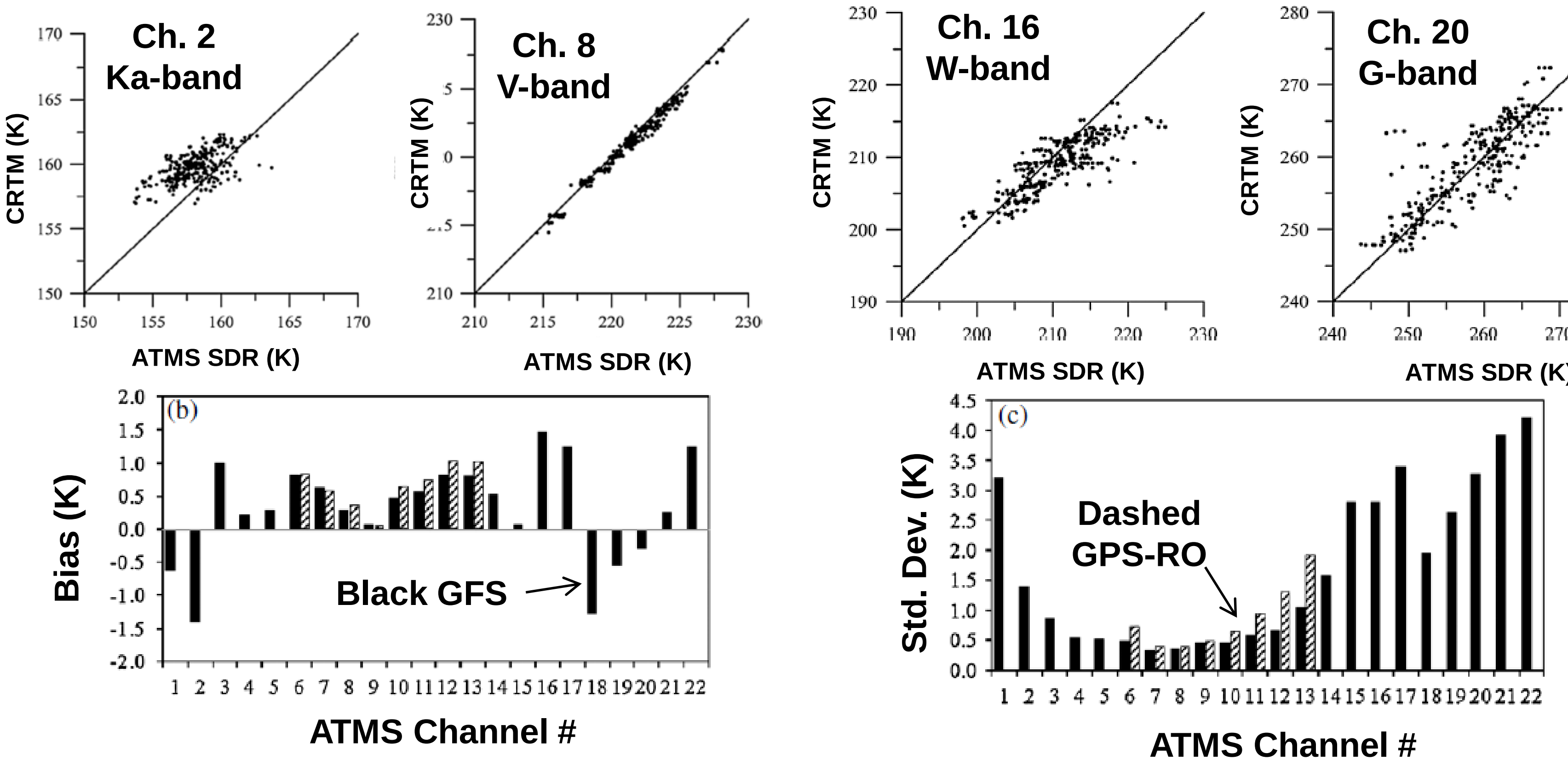

- Over ocean under dry, clear-sky, and calm conditions
- 20-26 December 2011
- Theoretical approach

JOURNAL OF GEOPHYSICAL RESEARCH: ATMOSPHERES, VOL. 118, 11,187–11,200, doi:10.1002/jgrd.50840, 2013

S-NPP Mission Cal/Val Campaign

10 May 2013 Sortie over Gulf of CA

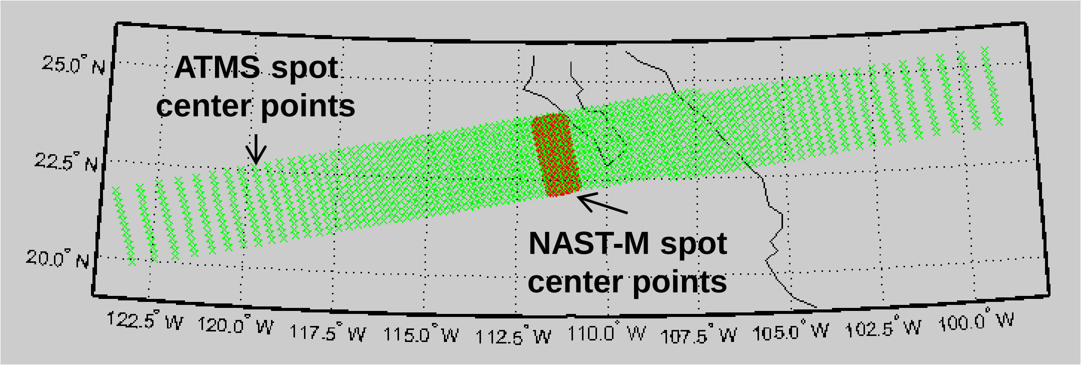

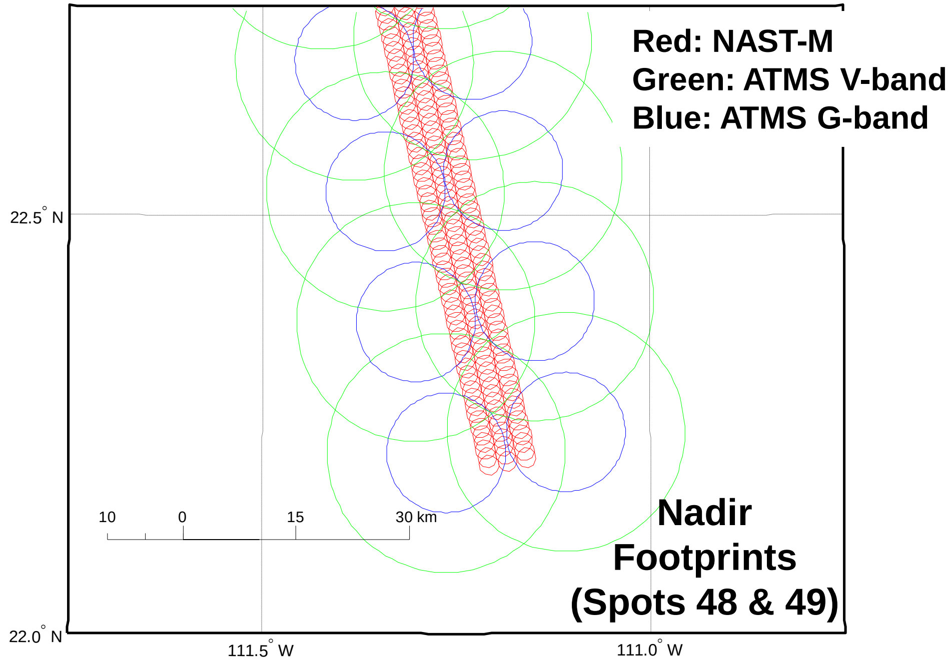

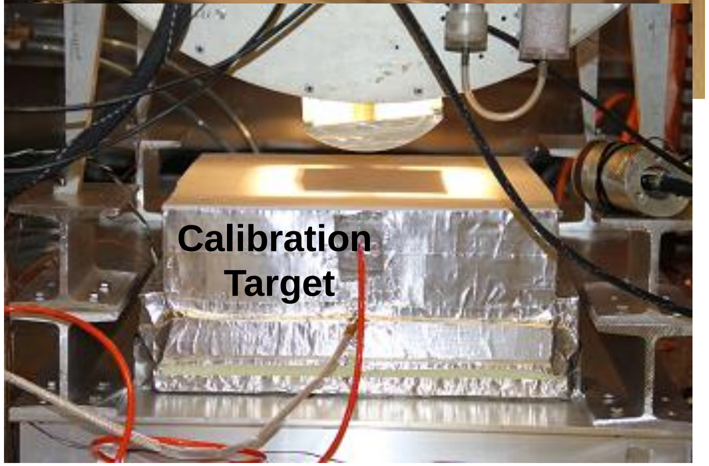

TDR-to-SDR Results: K and Lower V Band

Residuals of SDR and TDR against ECMWF/CRTM for May 24, 2013 over ocean and under clear skies

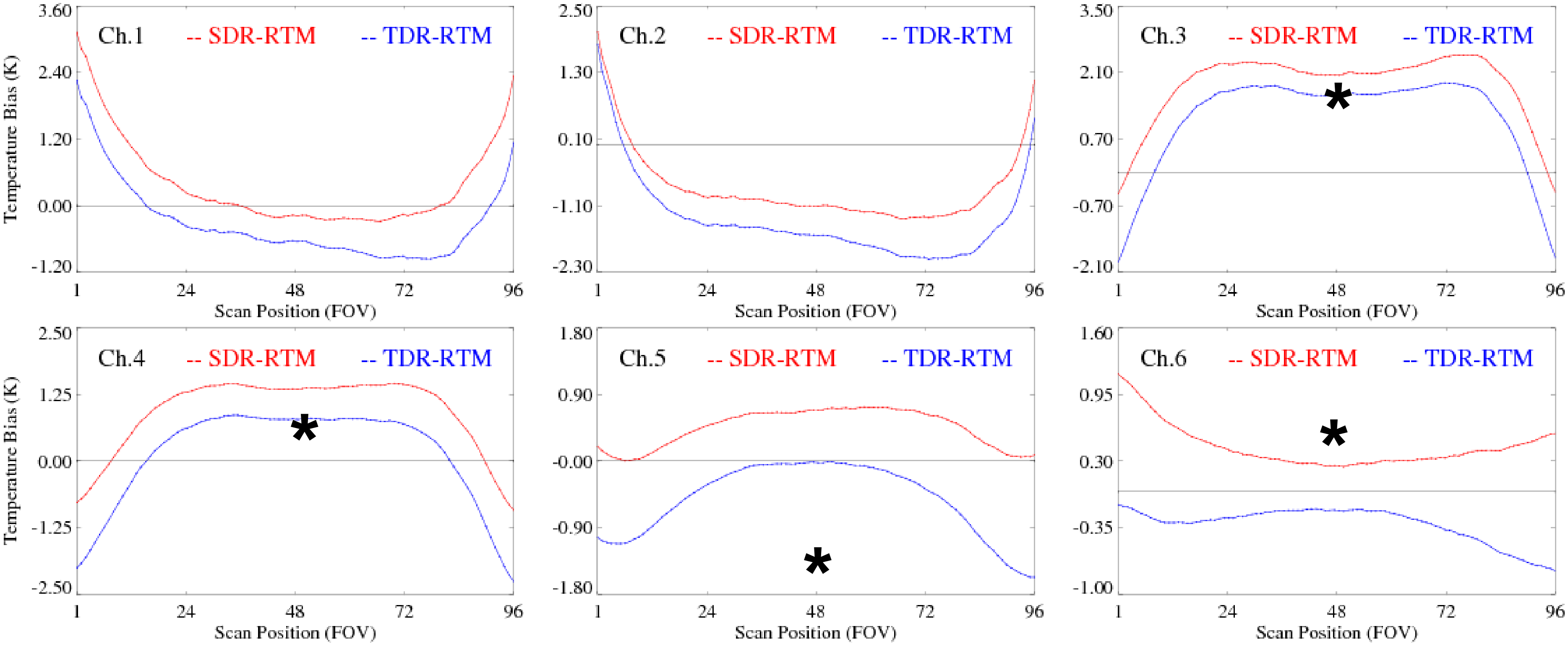

* **NAST-M Result from 10 May 2013; clear skies over ocean with limited # of high quality matchups**

TDR-to-SDR Results: Upper Air Sounding

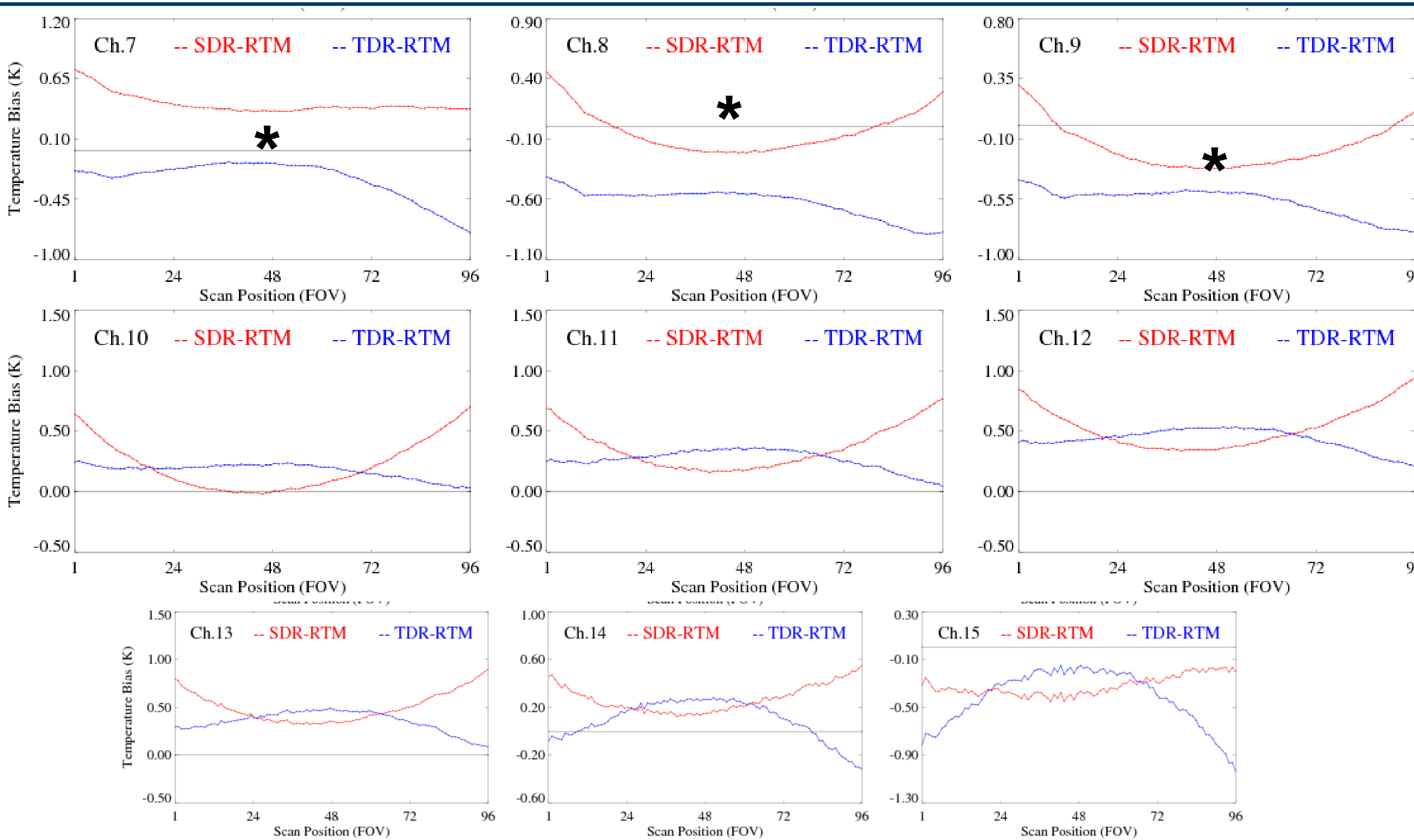

*** NAST-M Result from 10 May 2013; clear skies over ocean**

TDR-to-SDR Results for W/G Band

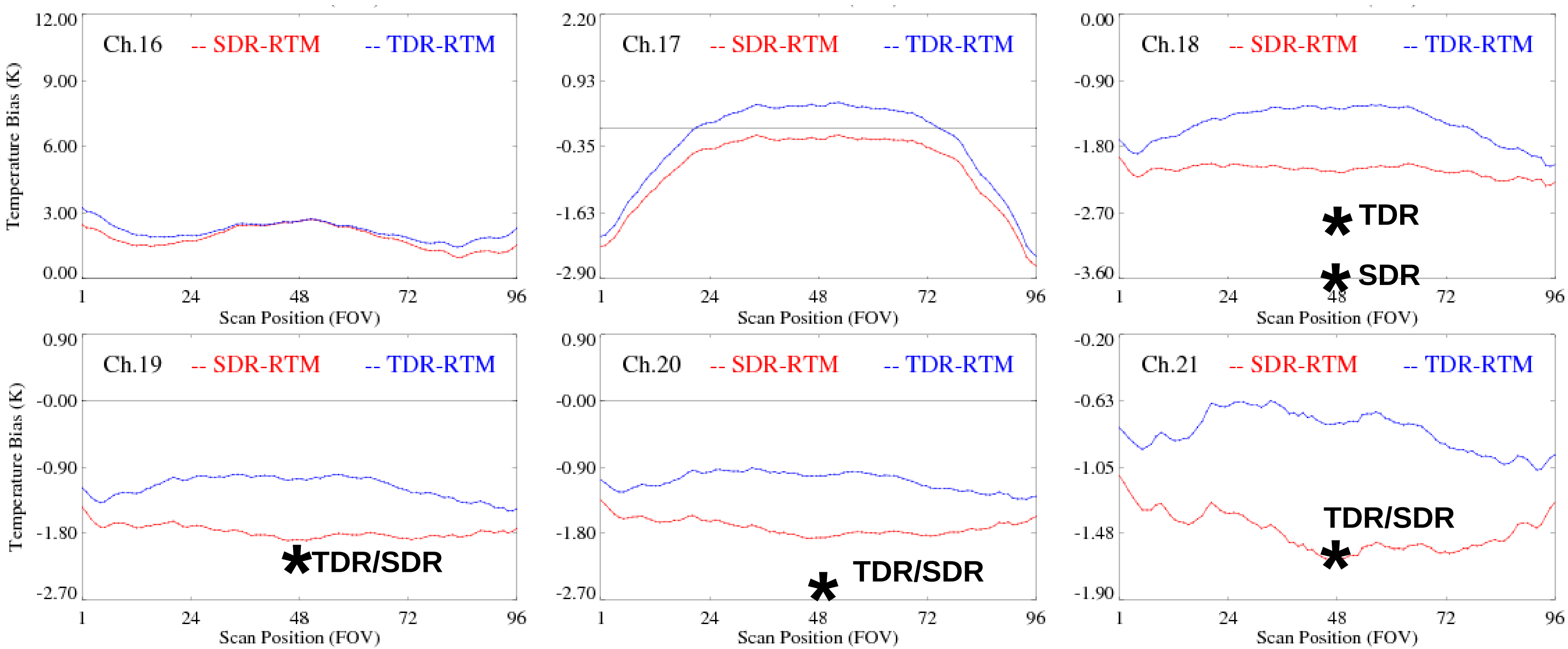

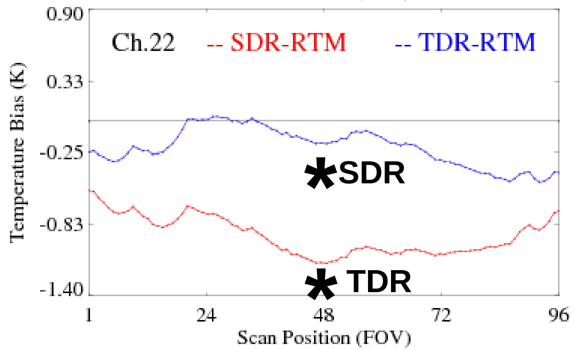

* NAST-M Result from 10 May 2013; clear skies over ocean with limited # of high quality matchups

LINCOLN LABORATORY
MASSACHUSETTS INSTITUTE OF TECHNOLOGY

S-NPP Pitchover Data Analysis & ATMS Scan Bias

S-NPP Pitchover ATMS Scan Angle Bias

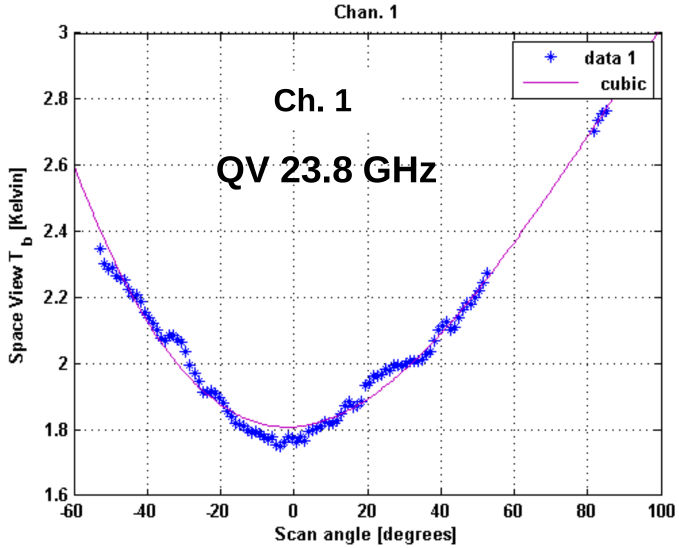

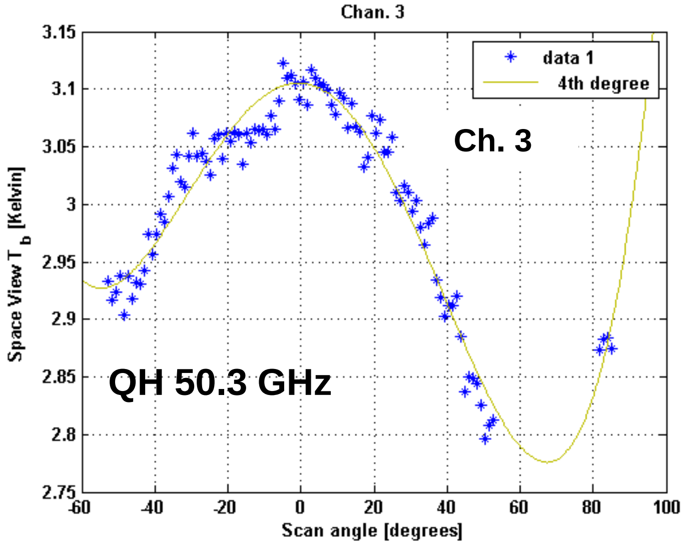

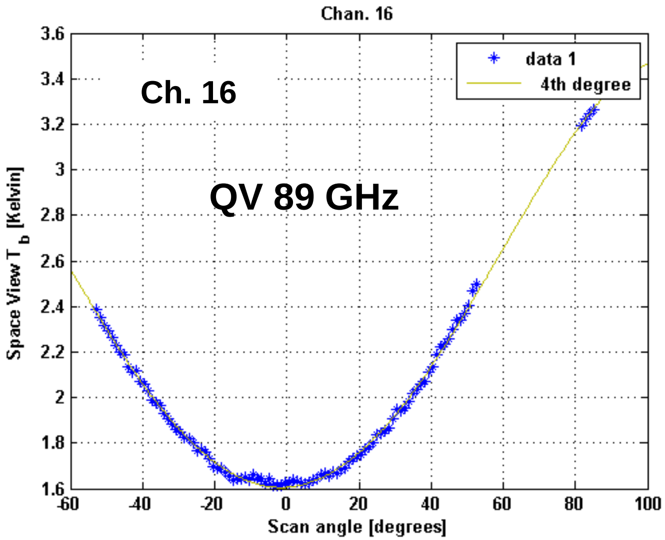

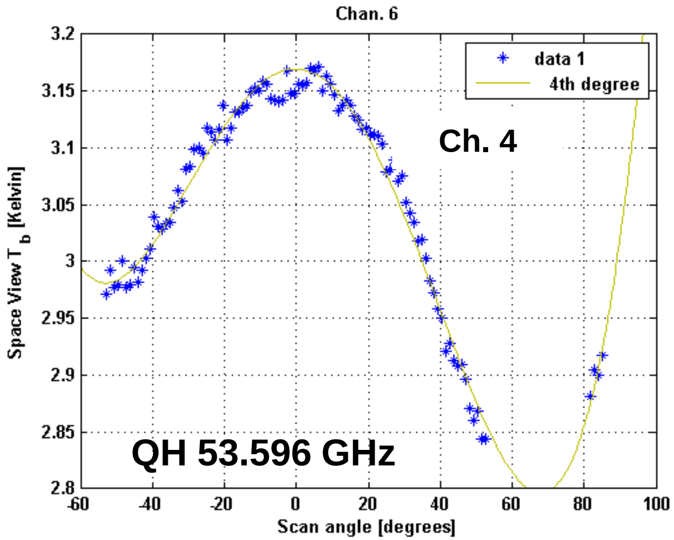

Potential Explanations

- With the Earthview sector viewing deep space, the radiometric scene is a homogenous and unpolarized source that fills the entire field of view of ATMS
- As an unpolarized scene, the polarization twist or cross-pol. impurity issues are not the primary explanation
- Alignment/pointing errors are unlikely due to strict subsystem quasi-optical alignment requirements that were verified during assembly
- Skimming or spillover is a possibility, but the bias symmetry is difficult to justify
- The bias asymmetry in the response is explained by near-field emission from the satellite, but the ATMS is positioned on the edge of the spacecraft, which doesn't justify the cosine or sine relationship

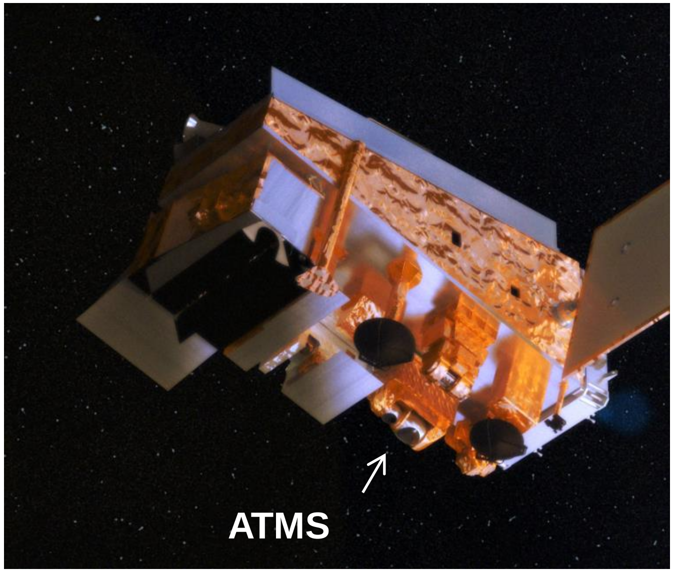

Potential Explanation: Flat Reflector Emissivity Model

- **ATMS scanning reflector is a gold-plated beryllium flat plate, oriented 45 degrees relative to the wavefront**
- **Conductive gold surface is a thin layer composed of microcrystalline granules, the emissivity can exceed the theoretical (Hagen-Rubens) emissivity of a perfectly flat bulk material**
- **The layered and rough surface is difficult to accurately model or simulate**
- **Values of the two polarization components can be expressed in terms of the normal emissivity derived from the Fresnel equations for reflections from a plane interface**
- **Reflector is scanned relative to a fixed linear polarization feed horn, the resulting Quasi-Vertical (QV) and Quasi-Horizontal (QH) components of emissions are scan angle-dependent (Eq. 1)**
- **Resulting antenna temperature in Equation 2**
  - ε_x is the quasi-V (QV) or quasi-H (QH) emissivity
  - T_{refl} is the physical temperature of the flat reflector

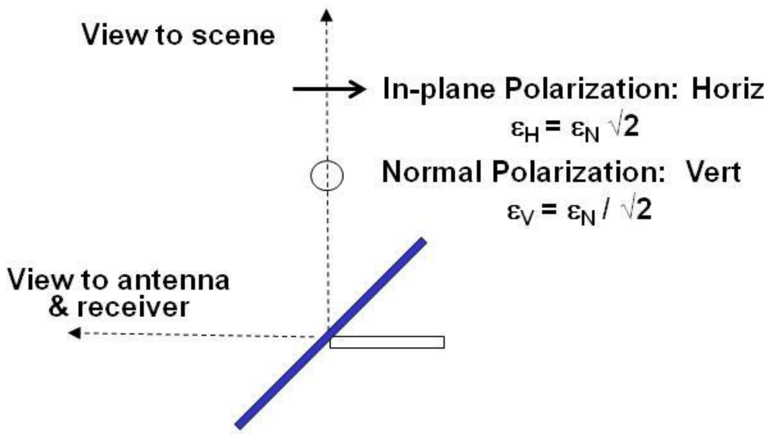

$$\varepsilon_{QV} = \frac{\varepsilon_n}{\sqrt{2}} \times \sin^2(\phi_{scan}) \quad \varepsilon_{QH} = \frac{\varepsilon_n}{\sqrt{2}} \times \cos^2(\phi_{scan}) \qquad (1)$$

$$T_{measured} = (1 - \varepsilon_x) \times T_{scene} + \varepsilon_x \times T_{refl} \qquad (2)$$

Kent Anderson (NGES)

On-orbit Derivation of the Normal Emissivity

- Swept the normal emissivity in a emissivity-corrected calibration algorithm until the Earth View Sector during the pitchover was flat
- Top figure presents the radiometric EVS results of stepping the emissivity for Channel 1
  - Cyan: original uncorrected result
  - Blue: corrected results at various emissivity steps
  - Green: tuned emissivity that had the lowest EVS standard deviation metric
- Bottom plot gives the derived emissivity for each channel
  - K- and V-band flat reflector is on the left
  - W- and G-band flat reflector is on the right
  - Tuning method was not sensitive to emissivity steps less than 0.05%
- Derived emissivity explained TVAC calibration anomaly

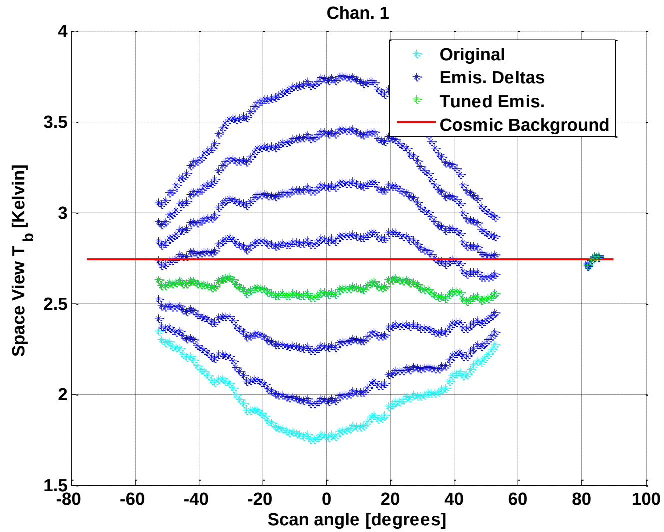

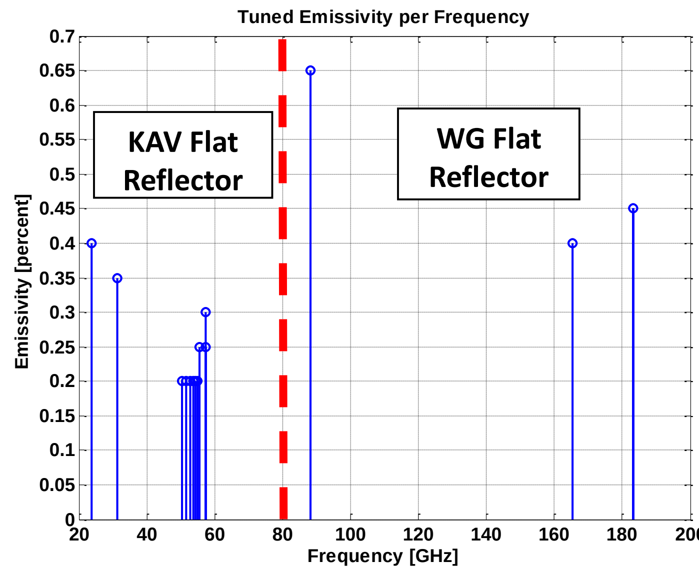

Future Work

- **TDR to SDR theoretical approach:**
  - **Review other options for derivation of eta (antenna pattern contributions), e.g., agree on use of W/G band measurements or utilize S-NPP roll maneuvers**
  - **Evaluate other options for modelling radiation sources like the opposite quasi-pol. and Earth radiation**
- **The TDR to SDR conversion in IDPS:**
  - **Enhance SDR algorithm to handle ocean and land surfaces separately for the scan bias correction**
  - **Investigate how the IDPS correction can implement the theoretical approach more accurately**
- **Flat reflector emissivity:**
  - **Characterize emissivity by measuring flat reflectors, which is presently underway at NGES**
  - **The TDR (not SDR) emissivity-corrected algorithm has been developed**
  - **The above corrected TDR algorithm needs to be implemented in IDPS and a LUT of coefficients added to the ATMS SDR PCT**

Backup Slides

Utility of the S-NPP Spacecraft Maneuvers

- **The S-NPP pitchover maneuver provided crucial data that is extremely difficult to replicate in pre-launch testing**
- **Pitchover data is helping characterize the scan bias on ATMS, and potentially providing insight into other heritage cross-track microwave instruments**
- **Pitchover data was used for the striping investigation to determine if the root cause was related to the scene radiance and for determining a striping metric**
- **Roll maneuvers provided value data for the selection of the ATMS space view sector**
- **Additional efforts are underway to utilize the roll maneuvers to characterize beam efficiency and scan bias**

ATMS Block Diagram

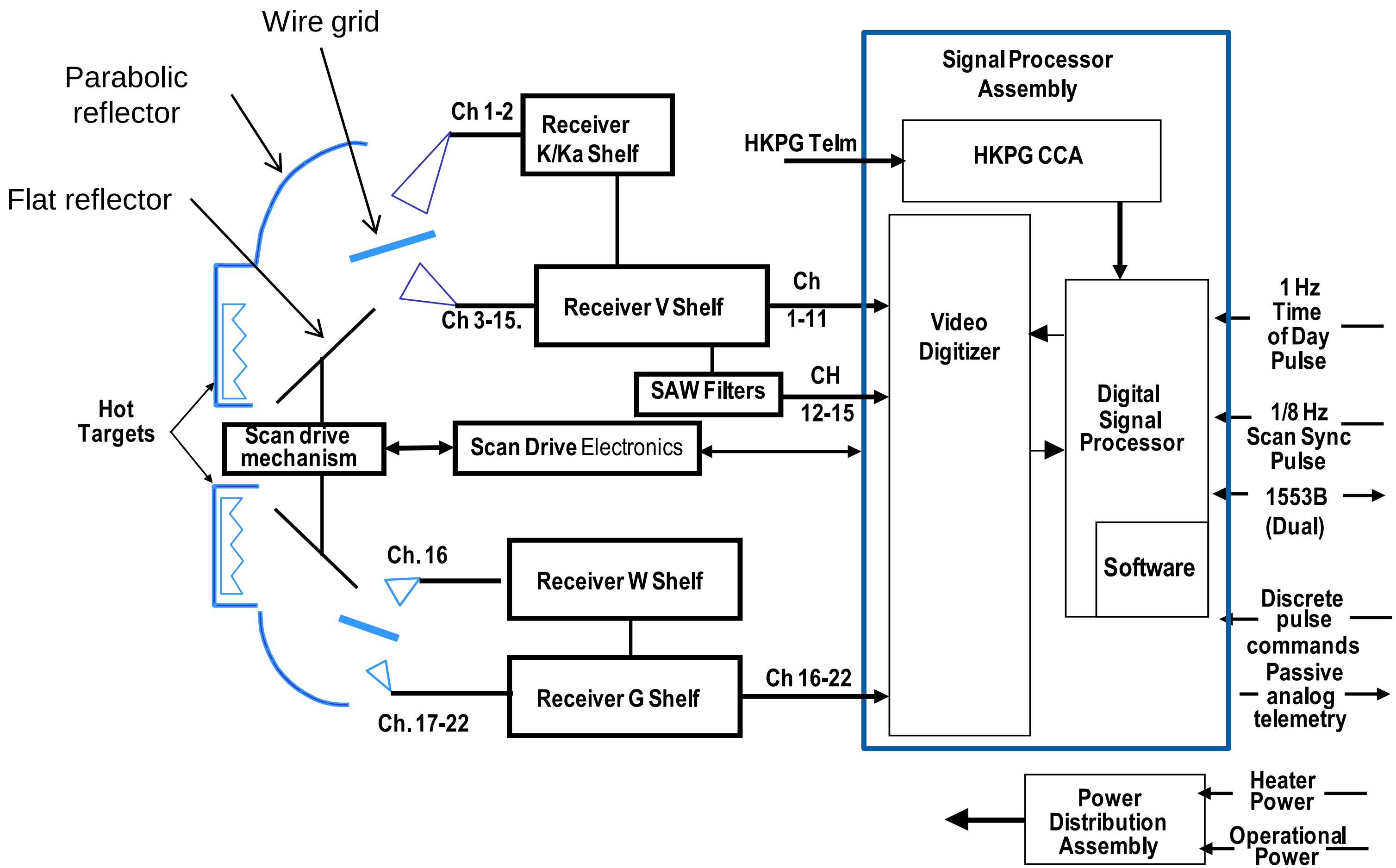

Estimating Contribution Parameters For Theoretical Expression

TDR **SDR** **Cosmic background is unpolarized**

$$T_a^{Qv} = \eta_{me}^{vv} T_b^{Qv} + \eta_{me}^{hv} T_b^{Qh} + \eta_{se}^{vv} E_b^{Qv} + \eta_{se}^{hv} E_b^{Qh} + (\eta_{sc}^{vv} + \eta_{sc}^{hv}) T_{c,RJ} + S_a^{Qv}$$

Assumptions & estimations

$$T_b^{Qh} = A^v(\theta) T_b^{Qv}$$

$$E_b^{Qv} = T_b^{Qv}$$

$$E_b^{Qh} = T_b^{Qh}$$

$$S_a^{QV} = \beta_0^v + \beta_1^v \cdot \sin^2(\theta)$$

$$S_a^{QH} = \beta_0^h + \beta_1^h \cdot \cos^2(\theta)$$

Solve for SDR in the above equation:

$$T_b^{Qv} = [T_a^{Qv} - (\eta_{sc}^{vv} + \eta_{sc}^{hv}) T_c - S_a^{Qv}] / [\eta_{me}^{vv} + \eta_{se}^{vv} + A^v (\eta_{me}^{hv} + \eta_{se}^{hv})]$$

Assumptions and caveats summarized next.

me **= main lobe earth;** ***se*** **= side lobe earth;** ***sc*** **= side lobe deep space**

Theoretical Expression's Assumptions & Caveats

- **The etas were calculated from the Compact Antenna Test Range measurements of the S-NPP ATMS antenna patterns**

- **The Earth T_b seen by the side lobe is approximated as the same as the main lobe Earth T_b** $E_b^{Qv} = T_b^{Qv}$

- **Because ATMS only measures a single quasi-polarization, the opposite polarization T_b was estimated as a linear estimate of the measured quasi-pol. T_b**

$$T_b^{Qh} = A^v(\theta) T_b^{Qv}$$

  - **Regression used ocean simulations (CRTM)**
  - **Regression was only applied to window channels (1-5 & 16)**
  - **Upper sounding and G-band channels used their measured quasi-pol. T_b instead**

- **The near-field satellite radiation was modelled using the S-NPP pitchover maneuver data**

$$S_a^{QV} = \beta_0^v + \beta_1^v \cdot \sin^2(\theta)$$

Sidelobe Intercept with Deep Space

- **Side lobe intercept of deep space was estimated using the CATR antenna pattern measurements**
- **G-band measurements at far angles (which side lobes would intercept deep space) was limited by noise floor of the CATR and set to zero**
- **W-band measurements of the cold space contributions resulted in unrealistic values and were not used**

Channel	$\eta_{sc}^{pp} + \eta_{sc}^{pq}$ (%)			T_c
	B1	B48	B96	
1	0.78	0.29	0.95	2.7645
2	0.49	0.36	0.76	2.7929
3	0.60	0.38	0.58	2.8964
4	0.52	0.42	0.57	2.9063
5	0.56	0.44	0.72	2.9135
6	0.60	0.35	0.63	2.9191
7	0.52	0.41	0.61	2.9248
8	0.53	0.40	0.66	2.9287
9	0.46	0.34	0.55	2.9328
10	0.35	0.22	0.48	2.9462
11	0.35	0.22	0.48	2.9462
12	0.35	0.22	0.48	2.9462
13	0.35	0.22	0.48	2.9462
14	0.35	0.22	0.48	2.9462
15	0.35	0.22	0.48	2.9462

Quasi-pol. Approximation

- **Simulated Ocean Radiances**
  - **CRTM (fastem v4)**
  - **US std atmosphere**
  - **5 m/s wind speed**
  - **290 K surface temp.**

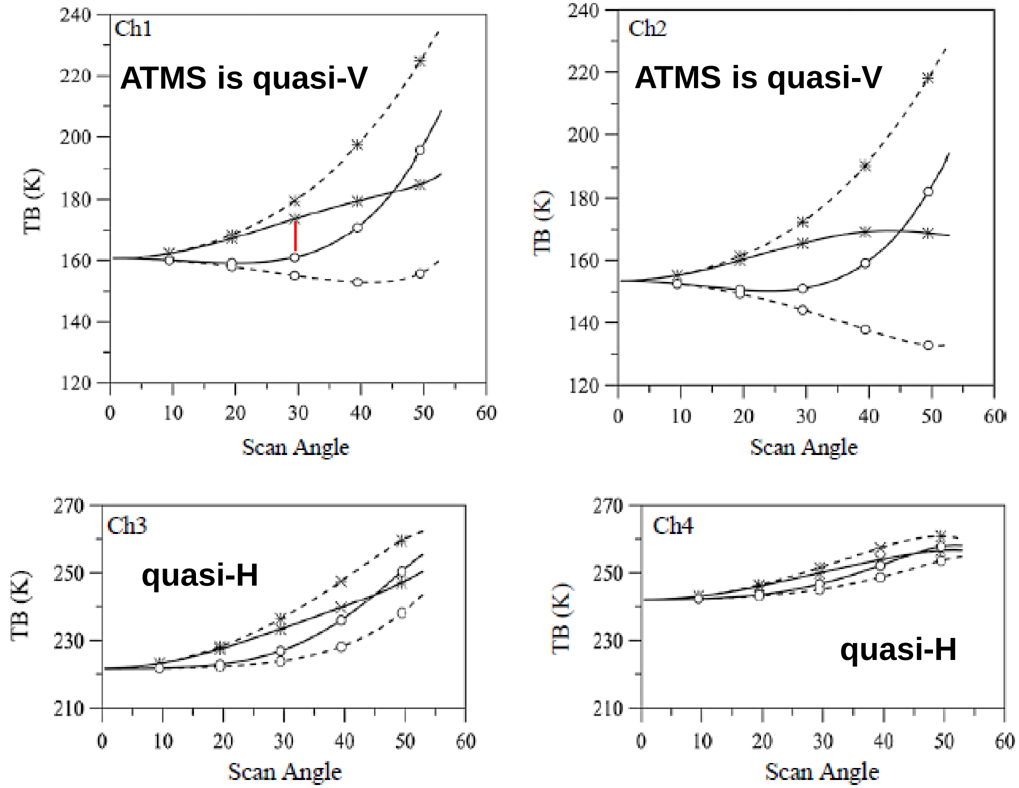

- **Linear regression between the two quasi-polarizations provided the conversion factor A(θ)**

$$T_b^{Qh} = A^v(\theta) T_b^{Qv}$$
$$T_b^{Qv} = A^h(\theta) T_b^{Qh}$$

- **Contribution in conversion:**

$$A^v(\eta_{me}^{hv} + \eta_{se}^{hv})$$

Ch.	$\eta_{me}^{pq} + \eta_{se}^{pq}$ (%)		
	B1	B48	B96
1	1.40	1.27	1.16
2	0.99	1.02	0.86
3	1.46	1.56	1.33
4	1.38	1.39	1.03
5	1.35	1.41	1.37

Circle = horizontal pol.
Asterisk = vertical pol.
Solid = quasi-pol.
Dashed = pure pol.

Implementing the Contribution Parameters in IDPS

TDR

SDR

$$T_a^{Qv} = \eta_{me}^{vv} T_b^{Qv} + \eta_{me}^{hv} T_b^{Qh} + \eta_{se}^{vv} E_b^{Qv} + \eta_{se}^{hv} E_b^{Qh} + \cancel{(\eta_{sc}^{vv} + \eta_{sc}^{hv}) T_{c,RJ}} + S_a^{Qv}$$

$$T_b^{Qh} = a(\theta) \cdot T_a^{Qv} + b(\theta)$$

$$E_b^{Qv} = T_b^{Qv}$$

$$E_b^{Qh} = T_b^{Qv}$$

$$S_a^{QV} = \beta_0^v + \beta_1^v \cdot \sin^2(\theta)$$

$$S_a^{QH} = \beta_0^h + \beta_1^h \cdot \cos^2(\theta)$$

Solve for SDR in the above equation (but with two changes above in red):

$$T_b = \left(T_a - S_a - (a \cdot T_a + b) \cdot \eta_{me}^{cr}\right) \Big/ \left(\eta_{me}^{co} + \eta_{se}^{co} + \eta_{se}^{cr}\right)$$

co = *vv* or *hh*
cr = *vh* or *hv*

Assumptions and caveats summarized next.

me = main lobe earth; *se* = side lobe earth; *sc* = side lobe deep space

Implementation Assumptions & Caveats

- **Differences from theoretical approach:**
  - **Side lobe intercept with deep space was removed**
  - **Opposite quasi-pol. of Earth sidelobe is treated as SDR** $E_b^{Qh} = T_b^{Qv}$
  - **Opposite quasi-pol. is estimated from measured quasi-pol. antenna temperature (instead of treating it as a brightness temperature)**

- **Parts that were kept the same as the theoretical approach:**
  - **The Earth T_b seen by the side lobe is approximated as the same as the main lobe Earth T_b** $E_b^{Qv} = T_b^{Qv}$
  - **Opposite polarization T_b was estimated as a linear equation of the measured quasi-pol. T_a (theoretical did use T_b)** $T_b^{Qh} = a(\theta) \cdot T_a^{Qv} + b(\theta)$
  - **The near-field satellite radiation was modelled using the S-NPP pitchover maneuver data** $S_a^{QV} = \beta_0^v + \beta_1^v \cdot \sin^2(\theta)$

Observations, Simulations and Angular Biases (CRTM & GFS/GPS-RO)

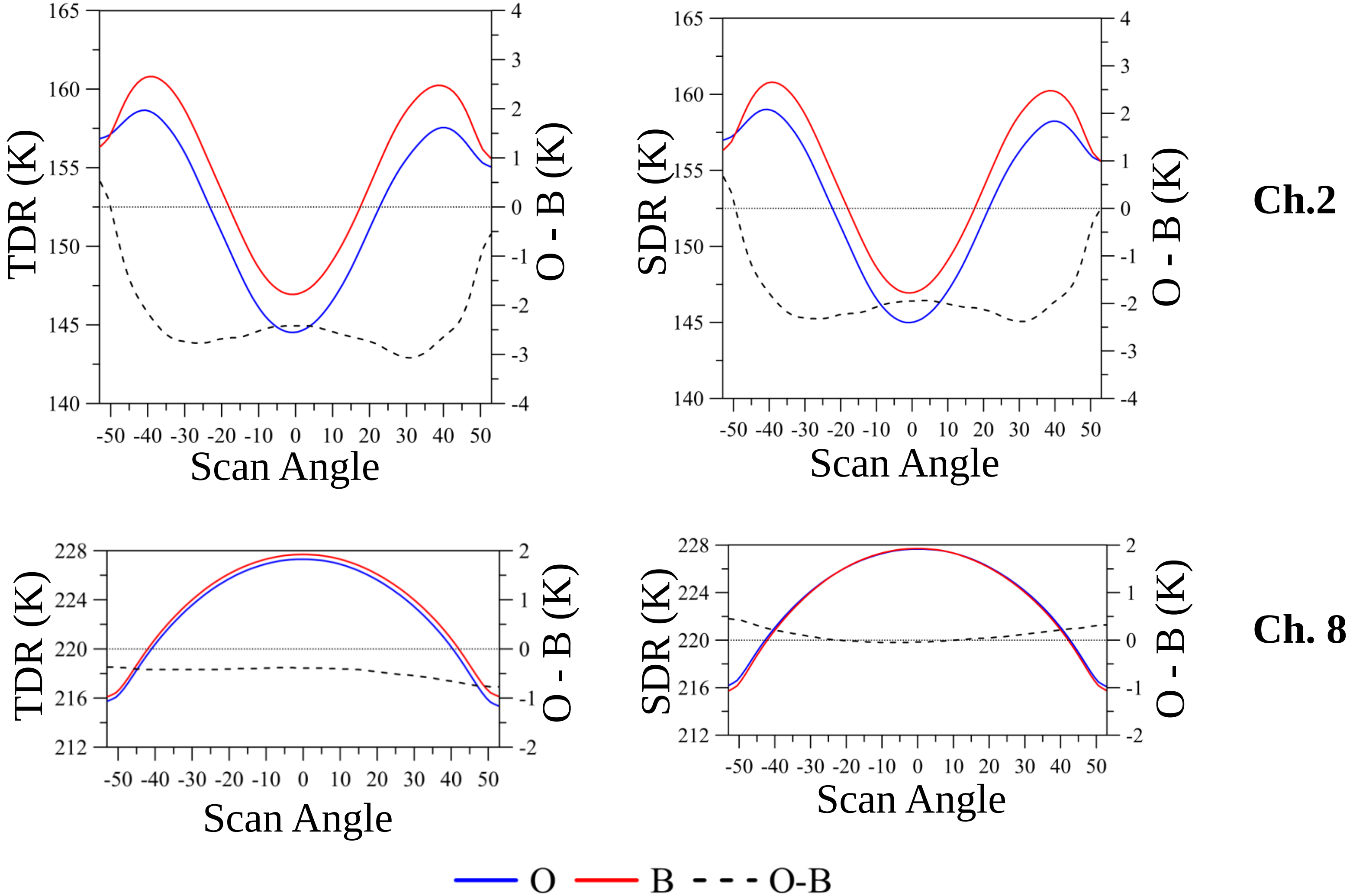

Radiance Versus Modeling Verification

Radiance to Radiance Comparisons

- Separate sensors measuring nearly the same point at the same time
- Examples include Simultaneous Nadir Observations (SNO) or aircraft underflights
- Pros: same atmosphere and surface conditions with similar instrumentation
- Cons: Different spectral or spatial characteristics and small data sets

Radiance to Model Comparisons

- Model the sensor and the atmosphere
- Examples include using state-of-the-art NWP, radiative transfer, and surface models
- Pros: large amounts of data
- Cons: Idealized or measured spectral or spatial characteristics; and modeling errors in the models

V-band ATMS vs NAST-M: 10 May 2013

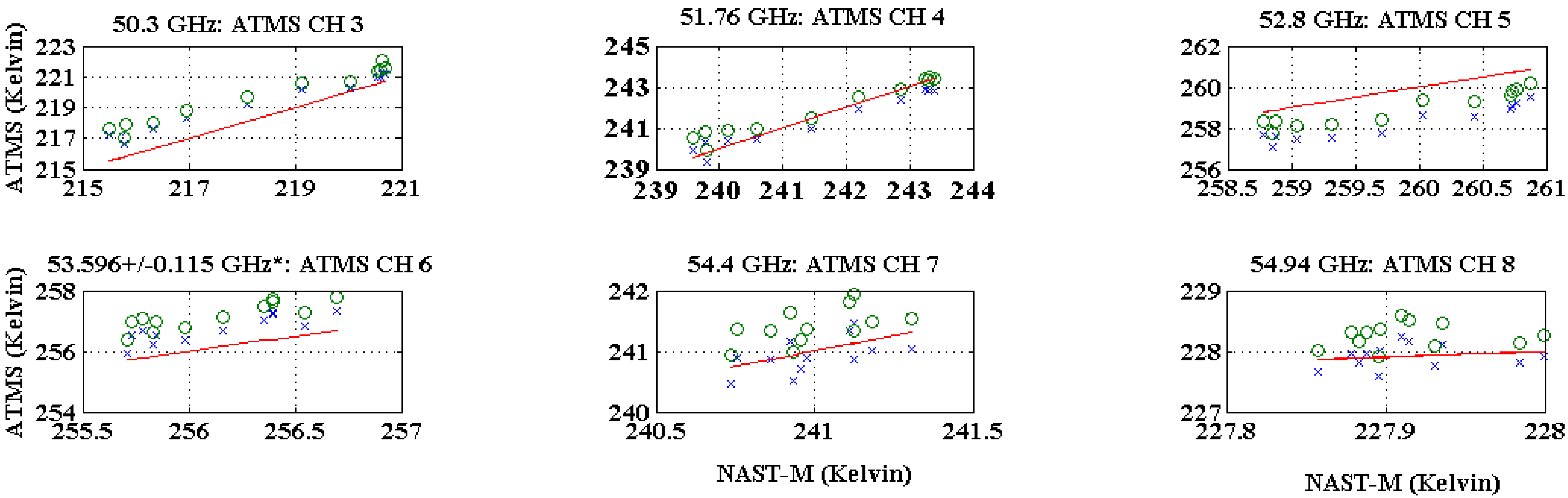

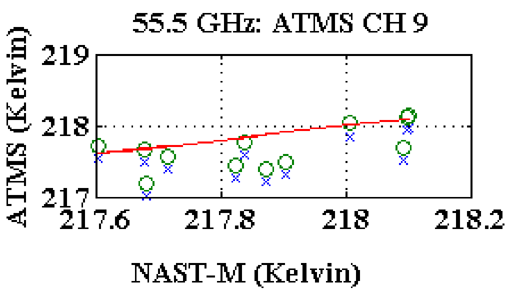

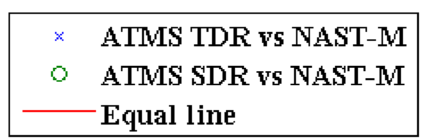

- **Used nadir spots only**
- **ATMS is the mean of spots 48 and 49**
- **NAST-M is the mean of spots 13, 14, 15**
- **For each ATMS "pseudo nadir spot," the average of all NAST-M spots are taken within the 2.2 deg. beam (31.6 km)**

G-band ATMS vs NAST-M: 10 May 2013

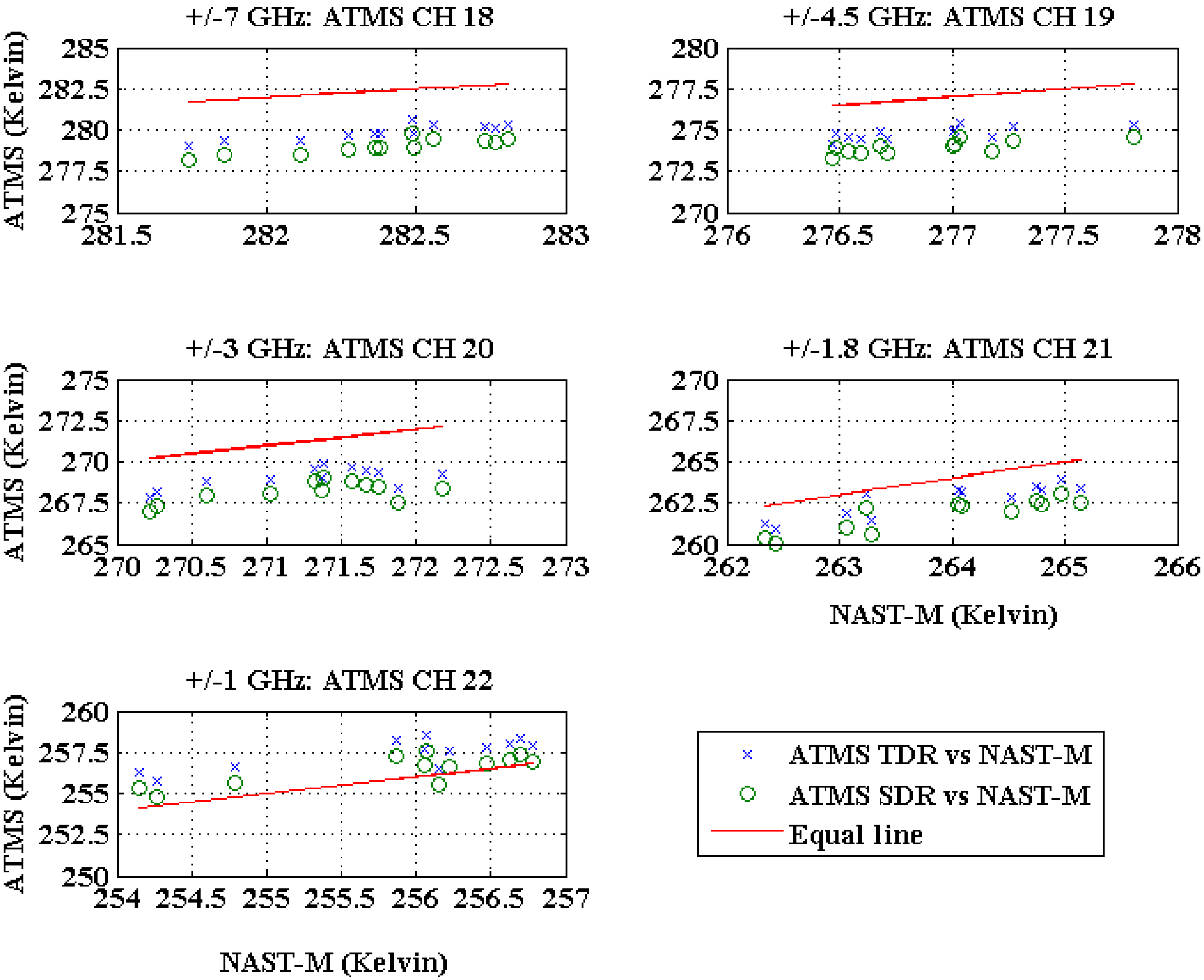

- **Used nadir spots only**
- **ATMS is the mean of spots 48 and 49**
- **NAST-M is the mean of spots 12 through 16**
- **For each ATMS "pseudo nadir spot," the average of all the NAST-M spots are taken within the 1.1 deg. beam (15.8 km)**

NOAA-14 MSU Deep Space Scan Bias

MSU Ch. 1 50.36 GHz

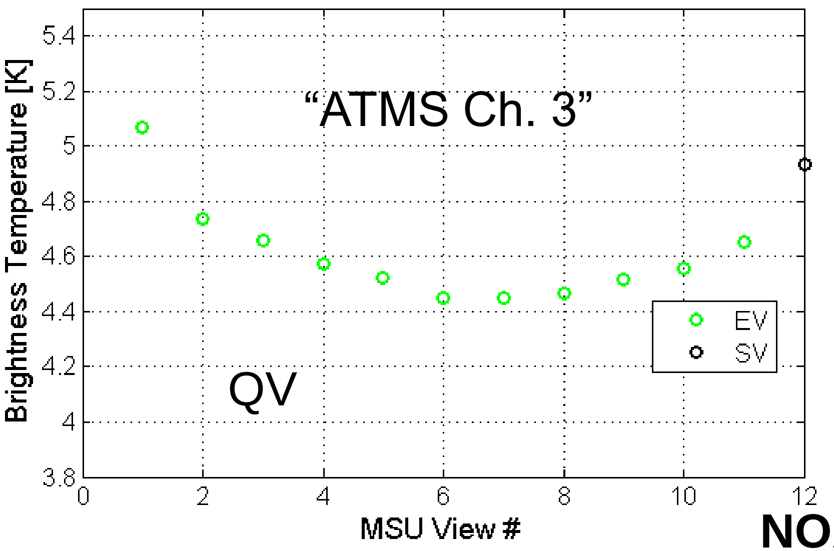

Ant. 1

MSU Ch. 2 53.74GHz

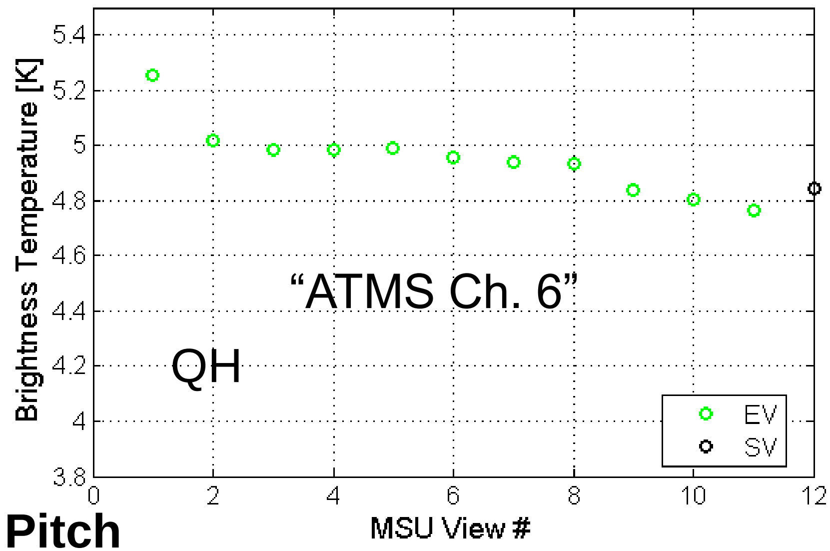

NOAA-14 Pitch Over Maneuver

MSU Ch. 3 54.96 GHz

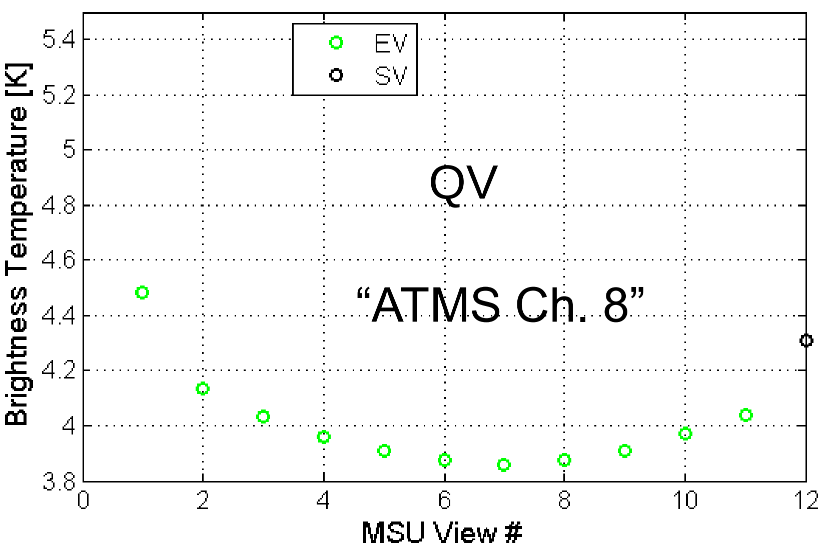

Ant. 2

MSU Ch. 4 57.95 GHz

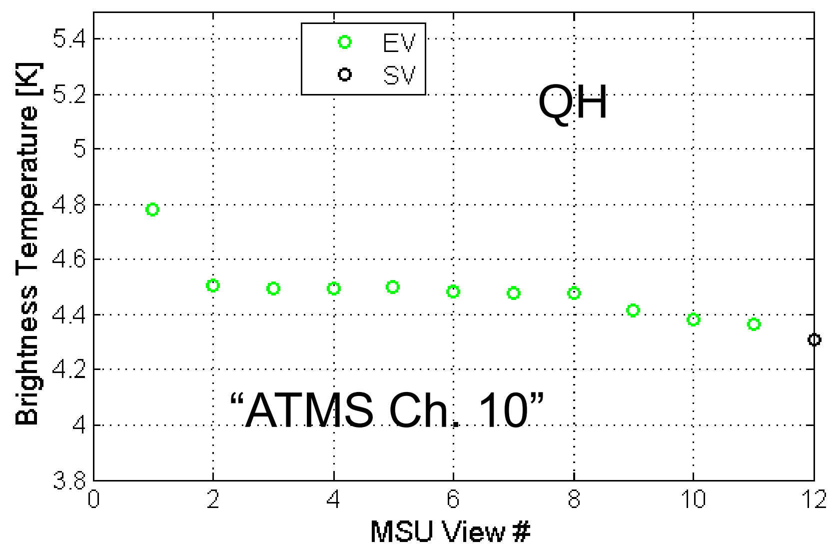

Emissivity Correction Parameters

- **First parameter is the physical temperature of the flat reflector**
  - **No temperature sensor is on the reflector, but used a nearby sensor on the scan drive mechanism**
  - **Calibration algorithm is fairly insensitive to the reflector temperature (i.e., temp. is multiplied by the emissivity), which was confirmed by a sensitivity study (i.e., adding 10° C showed marginal impact)**

- **Second parameter is the normal emissivity for each band (or channel)**
  - **Difficult to model or derive a theoretical equation**
  - **Plans are in preparation to measure angle-dependent emissivity on spare flight-like reflectors**
  - **Used pitchover maneuver to "fit" a normal emissivity value to each channel**

Calibration Algorithm Correction

Correction impacts three parts of the calibration equation:

$$T_{measured} = g \times (C_{scene} - C_{sv}) + T_{sv} \quad \text{(Eq. 3)}$$

SV = Space View

1. **The deep space radiometric counts are corrupted by the reflector's physical temperature and must be corrected in the deep space brightness temperature:**

T_{DS} = Deep Space T_b

$$T_{sv} = \rho \times T_{DS} + \varepsilon_{SV} \times T_{refl} = T_{DS} + \frac{\varepsilon_n}{\sqrt{2}} \times \sin^2(\phi_{SV}) \times (T_{refl} - T_{DS}) \quad \text{(Eq. 4)}$$

2. **Since the hot and cold calibration views are at different angles, the gain must be corrected for the reflector emissivity contribution:**

$$g = \frac{T_{HC} + \varepsilon_{HC} \times (T_{refl} - T_{HC}) - T_{sv} - \varepsilon_{SV} \times (T_{refl} - T_{SV})}{C_{HC} - C_{SV}} \quad \text{(Eq. 5)}$$

HC = Hot Cal (i.e., ambient)

3. **Finally, the scene brightness temperature is corrupted and this correction must be applied:**

$$T_{scene} = \frac{T_{measured} - \varepsilon_x \times T_{refl}}{1 - \varepsilon_x} \quad \text{(Eq. 6)}$$

ε_x is the quasi-V (QV) or quasi-H (QH) emissivity

K- & W-Band Error Plots (Kelvin)

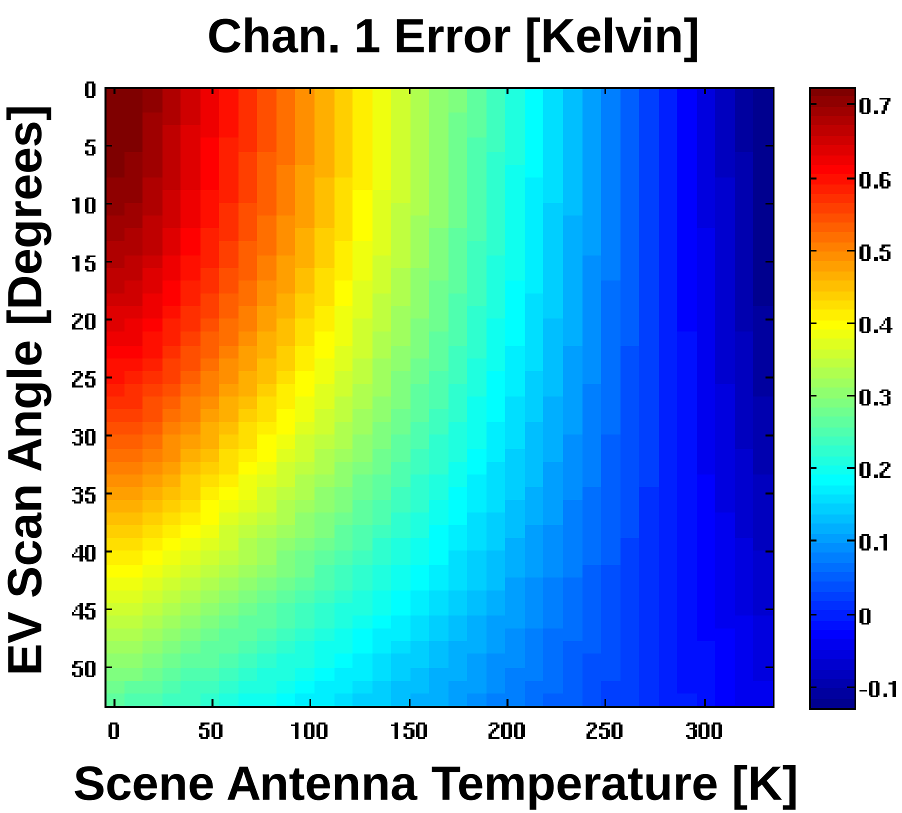

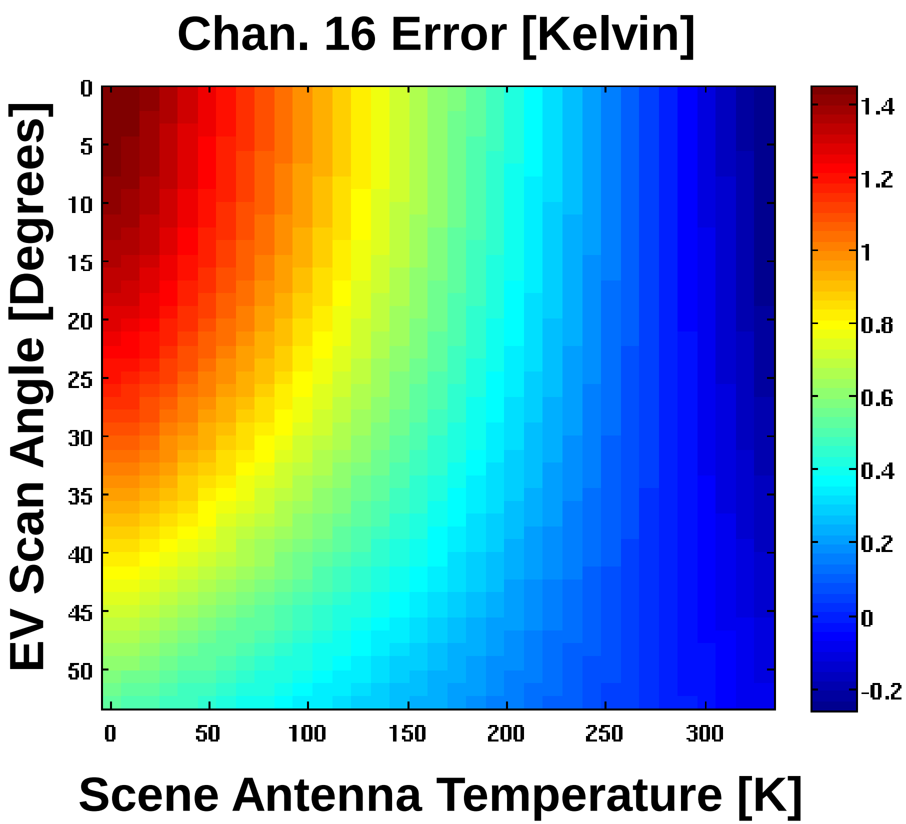

ICVS TDR Histogram ranges from 140 to 240 K
(no strong peak)
Worst case: ~0.4 K at nadir

ICVS TDR Histogram ranges from 200 to 280 K
(no strong peak)
Worst case: ~0.4 K at nadir

V- and G-Band Error Plots (Kelvin)

Chan. 3 Error [Kelvin]

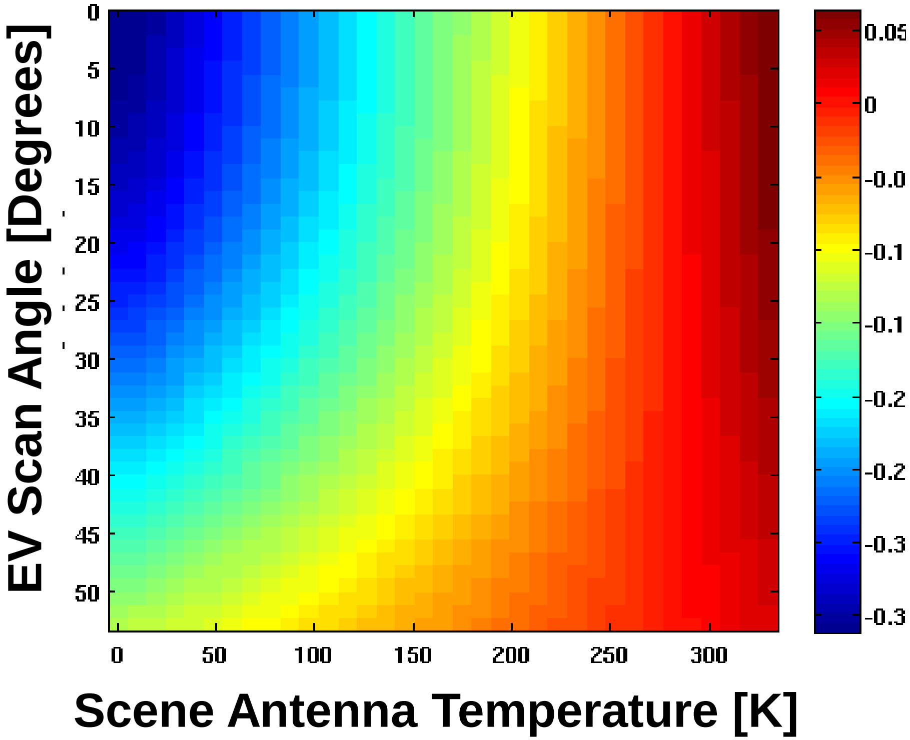

Chan. 17 Error [Kelvin]

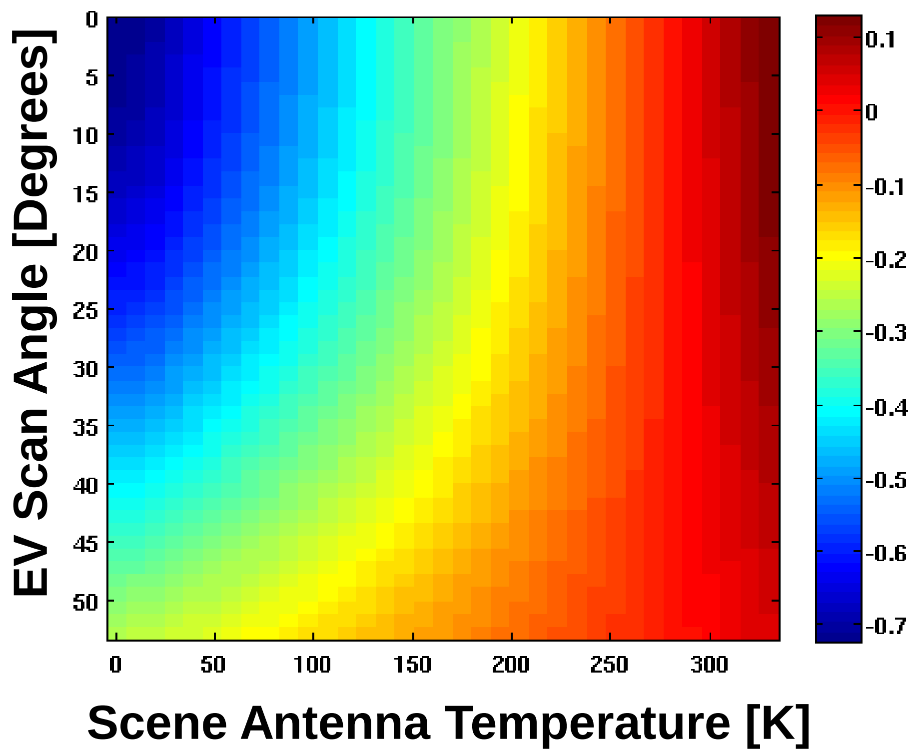

ICVS TDR Histogram ranges from 210 to 265 K (peak ~230 K)
Worst case: ~0.1 K at nadir

ICVS TDR Histogram ranges from 240 to 290 K (peak ~285 K)
Worst case: ~0.15 K

Applying Correction to Calibration Testing

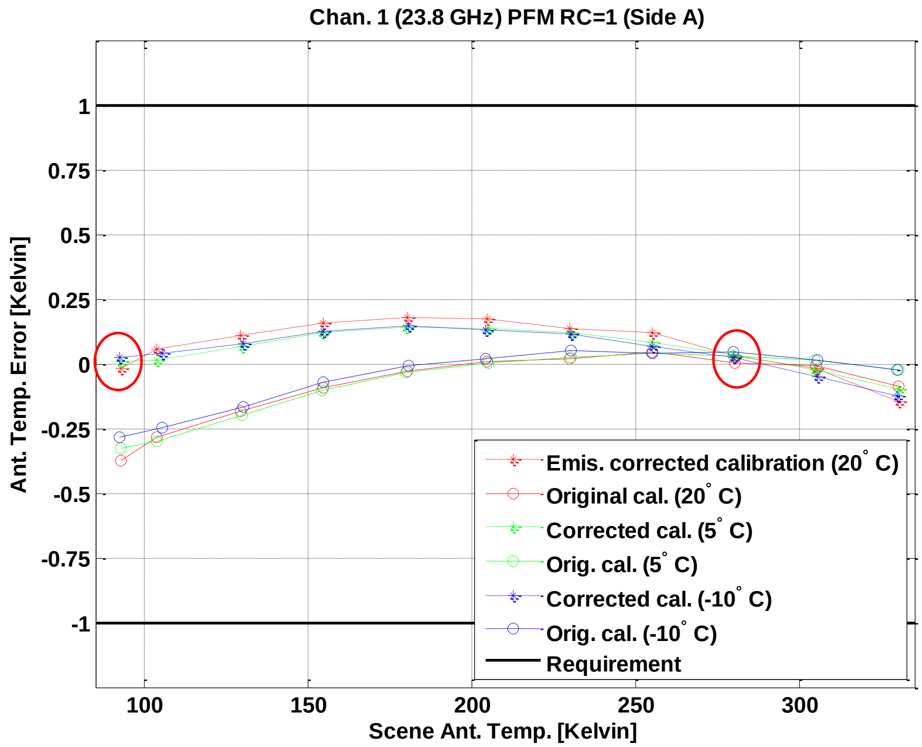

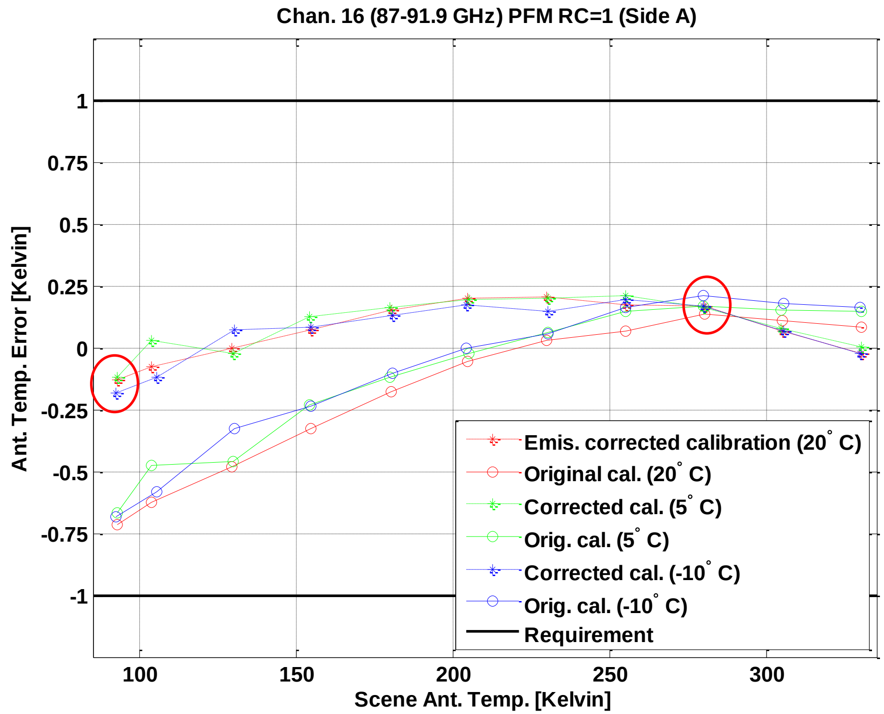

- **The error of quasi-V channels moved close to zero at the two calibration points**
- **V-band quasi-H channels also moved closer to zero**
- **Next chart shows W- and G-band results**

W- and G-Band Calibration Accuracy

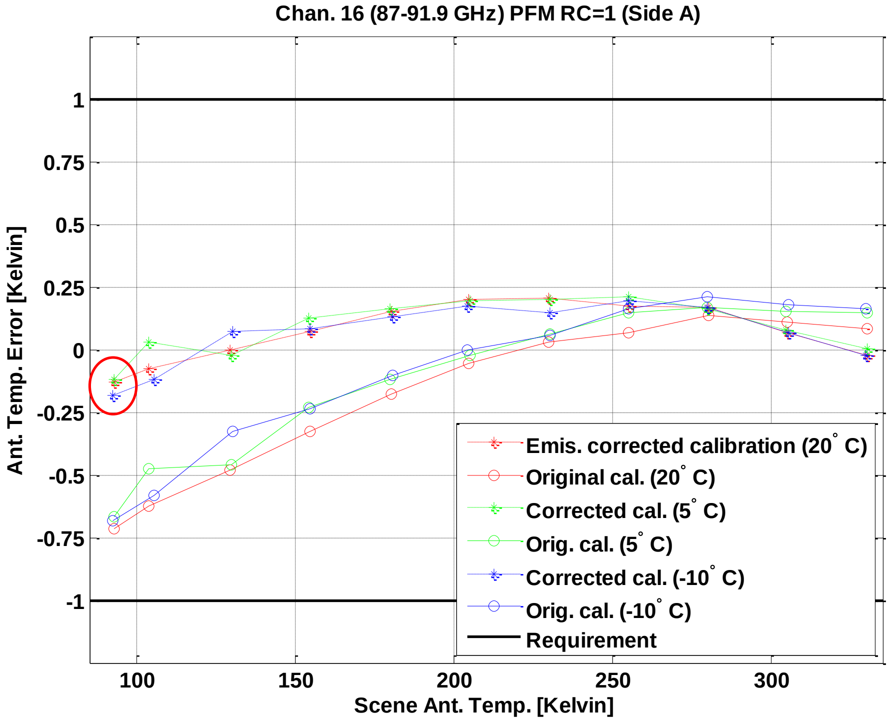

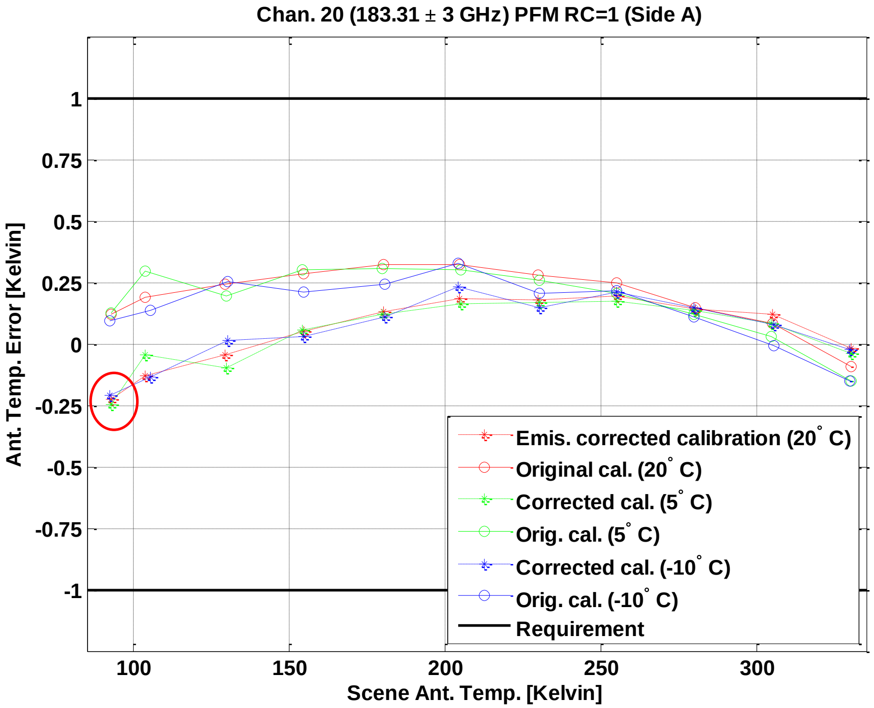

- **The two bands measuring the same external variable target now measure a similar radiometric signature after correction**
- **Analysis of external variable target indicates a ~1.3 K gradient across target, which might explain remaining cal. target discrepancy**

Nonlinearity Over Full Dynamic Range

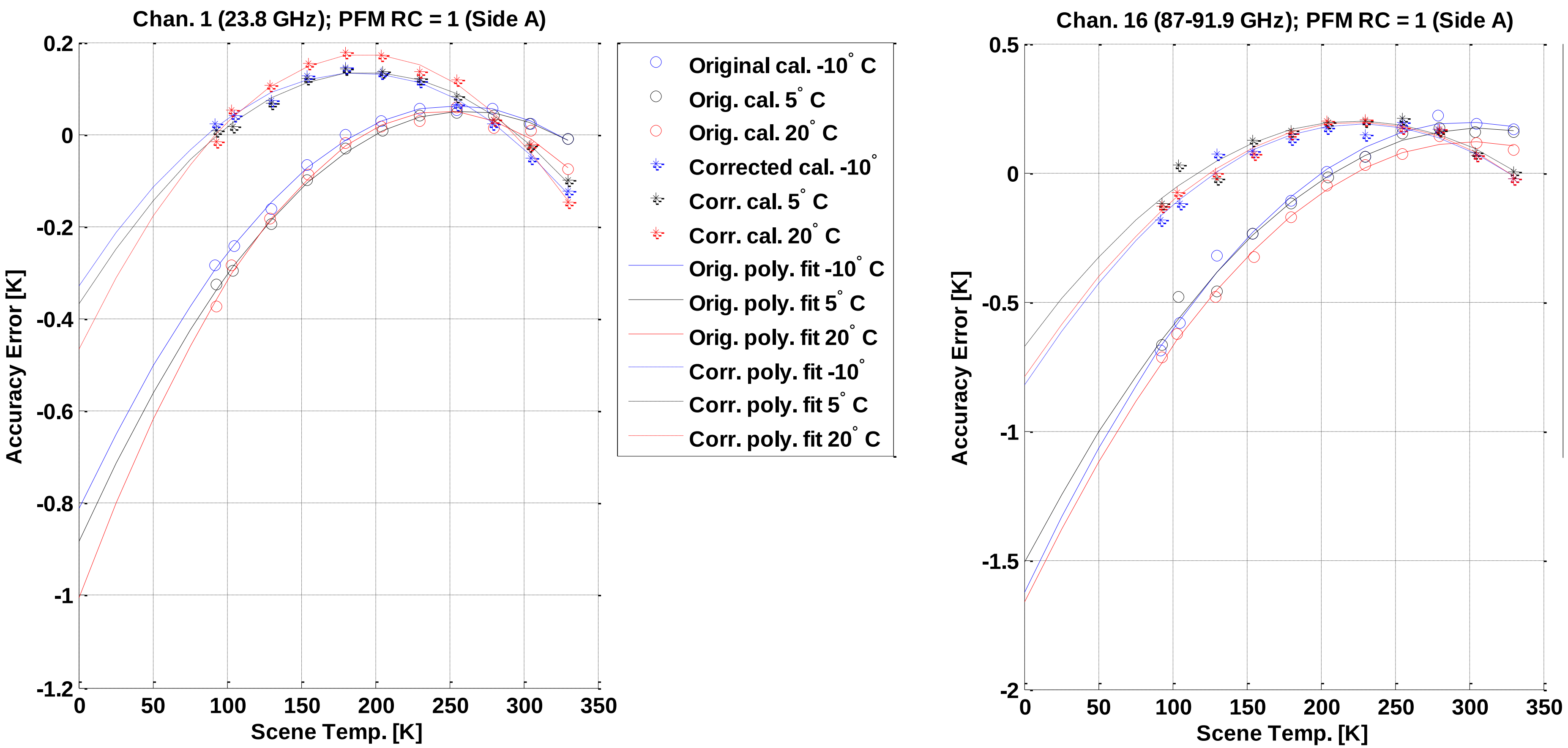

Did not significantly impact nonlinearity measurement

ATMS TDR-to-SDR Conversion

- **ATMS antenna temperature to brightness temperature conversion**
  - **NOAA STAR has identified a TDR-to-SDR conversion approach for ATMS utilizing:**
    - **Pre-launch antenna pattern measurements**
    - **S-NPP pitchover maneuver data**
  - **NOAA STAR implemented the conversion in the ATMS SDR Algorithm**
  - **Verified approach and implementation using:**
    - **CRTM & GFS/GPS-RO**
    - **CRTM & ECMWF**
    - **Aircraft measurements**
- **Investigating the S-NPP pitchover maneuver scan bias**
  - **Primary explanation is higher than expected flat reflector emissivity**
  - **Emissivity measurements under way at NGES**
  - **TDR algorithm correction prepared**
  - **Correction needs to be coded for IDPS**

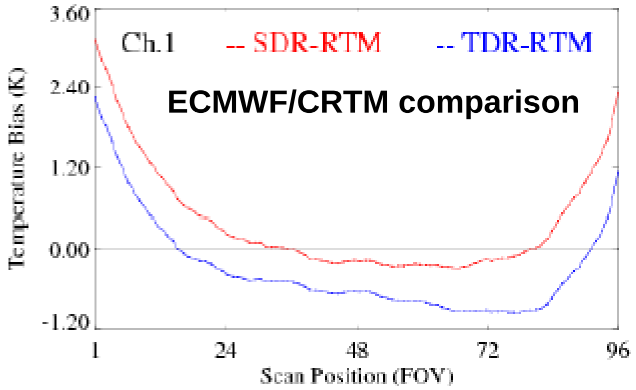

Emissivities derived from S-NPP pitchover maneuver